TRIBHUVAN UNIVERSITY

INSTITUTE OF ENGINEERING

PULCHOWK CAMPUS

THESIS NO:072/MSP/710

DEVELOPING A RESILIENT FRAMEWORK FOR EV CHARGING STATION THROUGH OPTIMAL INTEGRATION OF SOLAR PV, BATTERY ENERGY STORAGE (BES) AND GRID

BY

PRADEEP PAUDEL

A THESIS

SUBMITTED TO THE DEPARTMENT OF ELECTRICAL ENGINEERING

IN PARTIAL FULFILMENT OF THE REQUIREMENTS FOR THE

DEGREE OF MASTER OF SCIENCE IN POWER SYSTEM ENGINEERING

DEPARTMENT OF ELECTRICAL ENGINEERING

IOE, PULCHOWK CAMPUS

LALITPUR, NEPAL

JANUARY, 2026

COPYRIGHT

redited by University Grants
mission (UGC) Nepal 2020

Institute of Engineering
Electrical Engineering Department
Pulchowk Campus

त्रिभुवन विश्वविद्यालय
TRIBHUVAN UNIVERSITY
इन्जिनियरिङ्ग अध्ययन संस्थान
INSTITUTE OF ENGINEERING
पुल्चोक क्याम्पस
PULCHOWK CAMPUS
DEPARTMENT OF ELECTRICAL ENGINEERING
Pulchowk, Lalitpur

CERTIFICATE OF APPROVAL

The undersigned certify that they have read and recommended to the Institute of Engineering for acceptance, a thesis entitled "**Developing A Resilient Framework For Electrical Vehicle (EV) Charging Station Through Optimal Integration Of Solar PB, Battery Energy Storage (BES) And Grid**" submitted by **Pradeep Paudel** in partial fulfillment of the requirements for the degree of **Master of Science in Power System Engineering**.

Assistant Prof. Dr. Sujan Adhikari
Supervisor
Department of Electrical Engineering
Pulchowk Campus, Lalitpur

Dr. Sushil Aryal
External Examiner
Deputy Manager
Nepal Electricity Authority

Assistant Prof. Dr. Bishal Silwal
Program Coordinator
M.Sc. in Power System Engineering
Pulchowk Campus, Lalitpur

Assoc. Prof. Jeetendra Chaudhary
Head of Department
Department of Electrical Engineering
Pulchowk Campus, Lalitpur

Date: January 2026

ABSTRACT

Electric vehicle adoption in Nepal, where over 70% of new passenger vehicles are electric, faces a critical challenge. Analysis of the NEA Bharatpur charging station reveals grid outages during 3.31% of annual hours (290 hours) prevent EV charging, creating range anxiety and threatening adoption sustainability across Nepal's distribution network..

This thesis develops a resilience-oriented optimization framework integrating solar PV, battery energy storage (BESS), and grid connectivity for EV charging stations. Using 8,760 hours of real operational data from NEA Bharatpur charging station, a multi-objective Particle Swarm Optimization approach simultaneously maximizes Outage Coverage Probability (OCP) and minimizes Cost of Electricity (COE).

Analysis of four scenarios reveals grid-only systems achieve lowest cost (6.71 NPR/kWh) but zero resilience, battery-only reaches 90% OCP at 11.73 NPR/kWh, and off-grid proves infeasible (31.33% OCP, 25.59 NPR/kWh). The optimized PV-BESS-grid hybrid achieves 90% OCP at 10.09 NPR/kWh—14% cost reduction versus battery-only design—comprising 168 kW PV, 401 kWh BESS, and three 60 kW chargers, generating 234.85 MWh annually with 19.8% grid dependency reduction.

Pareto front analysis across eleven weight combinations maps the complete resilience-cost trade-off, identifying constrained knee-point at $w_1=0.6$ with maximum perpendicular distance (0.2983) among feasible solutions. Monte Carlo simulation (2,000 iterations) demonstrates 100% Outage Survival Probability for 1-hour outages (75% of events), 84.65% for 2-hour outages, and time-dependent performance: 96.24% (2h) during solar-assisted day periods versus 61.65% (2h) for battery-only evening operation.

MATLAB/Simulink validation confirms technical feasibility through power electronics modeling, demonstrating stable 800V DC-link regulation, successful MPPT operation, and seamless mode transitions. This research provides the first comprehensive resilience-cost optimization framework for Nepal's grid conditions, establishing actionable design principles supporting the country's 2031 complete vehicle electrification target.

ACKNOWLEDGEMENT

I would much like to thank my supervisor, Asst. Prof. Dr. Sujan Adhikari, Department of Electrical Engineering, Pulchowk Campus, who was patient, motivating, and supporting throughout the entire period in this thesis. His priceless advice, meaningful criticism, and unstopping support have played significant roles in the development of this study. I could not have thought of a more advisor and mentor.

My master's program is greatly indebted to Asst. Prof. Dr. Bishal Silwal, Program Coordinator, M.Sc. in Power System Engineering, Pulchowk Campus, who has provided assistance and counsel to me as an administrator.

I am extremely grateful to Mr. Sushil Aryal (External Examiner), Deputy Manager, Nepal Electricity Authority, to give his suggestions on this thesis work and to give constructive feedback.

I would like to acknowledge my great gratitude to Assistant Manager Mr. Bibas Acharya and Engineer Mr. Badri Pakurel, Nepal Electricity Authority, who kindly helped the research by offering the necessary data on operations and technical knowledge by which the basis of this work was built.

I would also like to express my gratitude to the Institute of Engineering Pulchowk Campus Department of Electrical Engineering, which gave me a chance to work on my thesis as a part of M.Sc. in Power system engineering.

I would like to give my heart-warming gratitude to all the professors and lecturers of the department whose invaluable suggestions and good-natured assistance were experienced during the thesis.

Finally and not the least, I would like to give my special thanks to my friends and family who were extremely supportive and cooperative throughout this journey.

Pradeep Paudel

072/MSP/710

January, 2026

Table of Contents

List of Figures

List of Tables

ABBREVIATION

AC	Alternating Current
AEPC	Alternative Energy Promotion Centre
BESS	Battery Energy Storage System
BMS	Battery Management System
CAN	Controller Area Network
CAPEX	Capital Expenditure
CC	Constant Current
CCS	Combined Charging System
COE	Cost of Electricity
CRF	Capital Recovery Factor
CV	Constant Voltage
DC	Direct Current
DOD	Depth of Discharge
DPP	Discounted Payback Period
EMS	Energy Management System
EV	Electric Vehicle
GDP	Gross Domestic Product
GHI	Global Horizontal Irradiance
IEEE	Institute of Electrical and Electronics Engineers
IGBT	Insulated Gate Bipolar Transistor
IRR	Internal Rate of Return
LCC	Life Cycle Cost
Li-ion	Lithium-ion
LSTM	Long Short-Term Memory

MOSFET	Metal-Oxide-Semiconductor Field-Effect Transistor
MPPT	Maximum Power Point Tracking
NDC	Nationally Determined Contribution
NOCT	Normal Operating Cell Temperature
NPR	Nepali Rupees
NEA	Nepal Electricity Authority
NPV	Net Present Value
NPC	Net Present Cost
OCP	Outage Coverage Probability
OPEX	Operational Expenditure
OSP	Outage Survival Probability
PBEVCs	Photovoltaic Battery EV Charging Station
PLL	Phase-Locked Loop
PSO	Particle Swarm Optimization
PV	Photovoltaic
PVGIS	Photovoltaic Geographical Information System
SOC	State of Charge
STC	Standard Test Conditions
THD	Total Harmonic Distortion
VSC	Voltage Source Converter

CHAPTER 1: INTRODUCTION

1.1 Introduction

The global transport system is rapidly transitioning to the supply of electric vehicles since it is one of the mass projects devoted to the minimization of the emission of greenhouse gases and climate objectives. Road transport is one of the largest portions of the entire energy spent and the overall volume of emissions generated, thus, electric cars (EVs) are one of the key technologies in the process of decarburization. In the recent years, global EVs have become popular with over 17 million EV vehicles sold in 2024 in a global basis of over 20 percent of total passenger vehicles globally. Specifically, large-paced growth causes the strain on a consistent and available network of EV chargers and fast charge stations, to facilitate their widespread implementation.

This is an international affair that is an exception in Nepal. Nepal, at that is an already developing state, was also among the most highly ranked in the world in terms of EV adoption in which over 70 percent of all new 4-wheel passenger cars imported to the country were electric by the year 2024. These transitions have been supported by good policy incentives as well as the high cost pressure/low electricity tariff. Similar to the situation in Nepal, however, grid power interruptions, which also require hours, have a severe impact on the precision of EV charging infrastructure. Although the implementation of the official abolition of the load shedding officially ceased to exist in 2018, a significant percentage of the energy is still inaccessible with most areas being infested with the hours of the unexpected and frequent energy shuts downs, including Chitwan, Bharatpur, and many others. Taking into account that most of the existing EV chargers stations are grid-driven, as well as the fact that grid service is not expanded to back-up power, charging cannot take place anymore when the grid coverage is lost, and causing the range anxiety to appear, and the level of confidence in electric mobility among their users to drop. In order to deal with such challenge, solar photovoltaic (PV), along with battery energy storage systems (BESS) is technically achievable as far as augmenting the resilience of charging stations goes. The solar PV technology can serve the local renewables and BESS is capable of saving energy and store the energy and can supply the energy during the grid outage in order to allow a charging station to generate itself during the islanded mode. On the other hand, the optimality of PV and

BESS when used in the PV stations to the EV fast charging stations in Nepal during grid outages was not well researched especially with the real outage and demand conditions benefiting the study. We prevent this deficiency of the current thesis, i.e. the resilience-oriented optimization model of EV fast charging station capacity, by having the optimal PV capacity, battery capacity, and fast chargers with the greatest possible Outage Coverage Probability (OCP), as well as, acceptable Cost of Electricity (COE); it is verified by a comprehensive modelling in MATLAB / Simulink.

1.2 Problem Statement

The adoption of electric vehicles is as high in Nepal as it has never been in any country; however, the reliability of EV charging stations is highly dependent on unscheduled, frequent power failures, which are triggered by disruptions in the transmission and distribution system, equipment failures, and disruptions caused by weather conditions. Even though the official technological state of load shedding is declared to be over, with a considerable proportion of battery owners, each day the duration of power cut would be many hours long, as the grid-dependent EV chargers lose all power entirely. This restricts the charging capacity and range anxiety among electric vehicle owners and economic playability of operating charging stations. The EV charging stations that exist in Nepal only run with the grid but there is no power supply at all. A possible alternative to gain reliable charging during the power outages is Solar Photovoltaic Generating System (PV) with the Battery Energy Storage System (BESS). PV is able to produce local energy during the day, whereas BESS can store power and produce during grid interruptions to allow gaps in grid connectivity to islanded operation. However, the PV-BESS dimension and control requirements of EV fast charging stations under the grid climate of Nepal that has frequent power cuts is not studied well yet. This problem is what this thesis will resolve by offering the resilience-first optimization framework of the PV-BESS integrated EV charging stations under the actual condition of grid power outages which will result in an optimization mechanism. It aims at identifying the most suitable PV and BESS power and working strategy along with providing outstanding continuity of charging service during power outage and low energy load required. The suggested methods are effective solutions with research support which would enhance reliability of EV charging in grid-inefficient regions such as Nepal. Currently majority of EV charging stations in Nepal operate on grid, meaning

that they do not have any other mechanism to support any back-ups. It refers to the fact that when the electricity is off, charging stations shut down, which makes the charging infrastructure insecure and increases range anxiety among customers of the EV segment. To ensure that permanent power of charging points is maintained with short-term power outages, installation of solar photovoltaic systems and battery energy storage systems are a precondition to the smooth operation of the charging to the grid. The solar energy plants are powered by solar PV to generate power on daylight and battery system to store power and provide power on the failure of the grid so that the charging stations can continue operating under charging to grid connected to grid as well as islanded operation. Nevertheless, recommendations on how PV-BESS should be sized and operate to power EVs in the grid of Nepal have not been made yet and the best sizing and ideal workings of PV-BESS system. The actual problem is maintenance of the charging service on an acceptable level in case of disruption. However, you can not make electricity costly. This is the proposed goal of this thesis as it would provide the solution to this issue and suggest a model of optimization of EV charging stations that would swell upon the principle of resilience but would depend on real-world outage trends in Nepal. The project will be set out to determine with high reliability at this level of voltage, the correct range of PV and battery size and operation plans, in the event of any power cuts, the charge stations are able to continue their service continuity so as to cause as minimal a cost as possible to the electricity. The future electric mobility of Nepal will be equipped with such an EV charging infrastructure capable of not only providing zero discontinuous service maintenance but also worth perceiving.

1.3 Objective

To design and test an efficient and cost effective hybrid energy structure of EV Charging station through the optimal combination of Solar PV, Battery Energy Storage (BES) and the/utility grid, utilization of the actual distribution system information and resilient based performance indicators.

Specific Objective:

- To characterize EV charging demand and grid outage behavior at Bharatpur Distribution Centre using real time operational data.

- To define and quantify resilience metrics, particularly Outage-Coverage Probability (OCP), for EV charging infrastructure.
- To formulate a multi-objective optimization problem that maximizes outage coverage probability (resilience) and Minimize cost of energy (COE).
- To optimally size PV and BES capacities using Particle Swarm Optimization (PSO).
- To model a grid-connected EV Charging station PV and BES, capable of islanded operation during grid outage.
- To evaluate system performance under outage and demand scenarios, representative of Bharatpur's distribution network.

1.4 Scope and Limitations

The current thesis has everything about the establishment of solid structure of grid based EV fast charging stations through integration of solar PV, battery energy storage systems (BESS) and utility grid in fluctuating grid conditions of Nepal. Using one full year (8,760 hours) of realistic data on EV charging need and grid outages at one of the representative NEA charging stations in Bharatpur, the work proposes and introduces a multi-objective Particle Swarm Optimization (PSO) model to effectively optimize the size of PV capacity, BESS energy capacity and the number of fast chargers within an optimal configuration. The model specifically emphasizes outage resilience, in terms of OCP and economic outcomes, in terms of COE. The optimal environment is simulated using large scale MATLAB/Simulink power electronics modeling including PV MPPT controller, bi-directional battery converters and EV charging interfaces/grid interfacing converters. In conclusion of this thesis, the size scheme has been proposed based on technical viability and economic evaluation, which resulted in an efficient design proposal of resiliency EV charging stations, which are applicable even to grid-unreliable regions such as Nepal.

The research is restricted to the level of EV charging station and does not include the possible impacts on the bigger grid distribution system, which is out of the area where the grid is connected. Other renewable options, like wind and micro-hydro, as well as alternative technologies to operate batteries, Vehicle-to-grid (V2G), are not considered in this analysis. The proposed framework is not simulated by any hardware or

hardware-in-the-loop simulations and hardware implementation, and its validation is solely achieved through MATLAB/Simulink based simulations and does not test the performance of the framework in practice.

CHAPTER 2: REVIEW OF LITERATURE

2.1 Overview

Due to the rapid increase in the electric vehicle adoption in different parts of the world, the stability of EV charging systems has become a research issue of concern. EV charging systems, integration of renewable energy, and battery energy storage systems are discussed in the comprehensive literature, but the particular issue of resilience of charging stations during the frequent grid outages has been comparatively overlooked, particularly in the developing countries. The chapter is a systematic review of the related literature in four interdependent areas namely: Power system resilience and outage-oriented metrics.

- PV-BESS integration for resilient energy systems
- EV charging station architectures and power electronics interfaces, and
- Optimization techniques for PV-BESS sizing incorporating resilience considerations.

2.2. Power System Resilience and Outage-Oriented Metrics

The resilience of power systems has been described as the capacity of an energy system to forecast, overcome, adjust to, and recuperate swiftly to the disturbances which include faults, adverse weather conditions, and equipment failures. In contrast to other metrics of reliability (SAIFI, SAIDI) in which the operation of the system during and after an outage is considered, resilience-oriented metrics are explicitly determined by the system and its properties.

A unique study on resilience evaluation of PV-battery systems has been given and the idea of self-sustainment period of buildings when there is no grid has also been introduced [1]. The possible continuity during different periods of outage was estimated in the work of simulating over 100,000 outage scenarios. This study has shown that a significant effect of battery capacity on outage survivability; nevertheless, EV charging time-dependent loads were not considered.

The resilience analysis has been incorporated into a hybrid framework that is data driven, whereby Monte Carlo outage simulation has been combined with machine-learn-based load and solar forecasting [2]. The need of historical outage traits in the

resilience planning was introduced in this work, and it was demonstrated that optimization-based sizing can enhance outage performance. Nonetheless, microgrids and building loads were analyzed instead of EV charging stations that have another demand profile.

The topic of resiliency in EV charging stations was specifically discussed in which solar PV, standby batteries, and grid supply were coupled with robust control systems [3]. The study demonstrated that hybrid energy systems could be charged without interruption in the case of grid failure but system resilience was evaluated primarily based on instantaneous efficiency and voltage stability measures instead of probabilistic outage coverage measures.

On the whole, these sources indicate that, although the assessment methods of resilience have been thoroughly developed in terms of buildings and micro grid, the resilience measures of charging stations including measures directly determining the coverage of demand during outage events, are not well studied.

2.3 PV and BESS Integration for Resilient Energy Systems

Combined deployment of PV generation and battery energy storage systems has been commonly explored with regards to its contribution to energy self-sufficiency and energy resilience. It was surveyed by installing PV battery systems in non-off-grid healthcare centers in outage-prone locations and it was demonstrated that battery-based PV systems bring a significant decrease in energy, which is not dispatched during grid outages [4]. The same was done with new resilience parameters of PV-battery systems and old reliability parameters were developed and old estimates on outage risk underestimation [5].

In grid-connected systems, appropriately sized PV-BESS systems can not only reduce grid dependency, but could also increase load supply continuity [6] [7]. It was emphasized in these works that PV alone cannot be used to provide resilience because of intermittency, and the outage performance of battery sizing is critical. However, the majority of PV–BESS research has been on building or micro grid of comparatively constant load profiles. EV fast charging stations are, however, typified by large power ratings, infrequent arrivals, and strict conditions on continuity of service, which means that the sizing techniques at the charging-station level are necessary.

2.4 EV Charging Station Design and Power Electronics Interfaces

A typical grid-connected PV-BESS EV charging station employing DC buses was designed and minimized conversion losses as well as enhanced control flexibility, in comparison to standard designs, were demonstrated [7]. Though converter-level simulations and control strategies were described in detail in these studies, the studies focused primarily on transient-level performance, efficiency, and voltage regulation, not on the long-term behaviour and recoverability of power failure and recovery.

Various researches have been examined regarding technical architecture of PV BESS embedded EV charging stations. Battery-based and PV-based hybrid-source EV charging systems were introduced where emphasis was laid on the use of bidirectional DC-DC converters to charge and discharge batteries [8] [9]. Bidirectional buck-boost DC-DC converters have found significant applications in charging and storage of EVs because they can control both ways with minimal components and high efficiency [8] [10] [11].

2.5 Optimization Techniques for PV-BESS Sizing

The optimization of photovoltaic (PV) generation, battery energy storage systems (BESS) and charging infrastructure in EV charging stations has been determined to be a nonlinear and multivariate optimization problem. This complexity is accompanied by varying solar irradiance with time, non-deterministic demand of EV charging, non-deterministic state-of-charge of batteries, ambiguity in grid blackouts, and integrated techno-economic limits. In turn, the literature has adopted a large variety of optimization methods that embrace Mixed Integer Linear Programming (MILP), Genetic Algorithms (GA), Differential Evolution (DE), and Particle Swarm Optimization (PSO).

Nevertheless, the classical optimization methods (MILP, etc.) are most efficient when formulating the problem is a convex and linearized problem; there needs to be substantial simplification to battery dynamics and outage behavior to be done and thus these methods cannot be applied to resilience-oriented research [2]. Consequently, evolutionary algorithms like GA and DE have been extensively used to solve the problem of PV-BESS sizing because they integrate nonlinearities and discrete decision

variables. However, these methods are often linked with slow convergence and large parameter tuning needs especially in long time-series simulations.

The initial algorithm introduced by Kennedy and Eberhart is the Particle Swarm Optimization (PSO) that has been identified as an apt optimization method to use with renewable energy system sizing because it is simple in design, converges quickly, and has the ability to search globally [6]. PSO is a metaheuristic that is population based and modeled after the social behavior that is witness in the flocking of birds and schools of fish. A possible combination of system design variables is specified in PSO, and it is known as a particle. Updates on individual and globally best solution of the swarm are used to determine the movement of particles in the search space.

A multi-agent PSO-based optimization model of PV-BESS-based EV charging stations was introduced whereby the minimization of system cost was effectively established and the EV charging demands were met under renewable intermittency [6]. In their work, the utility of the PSO in the joint optimization of the PV capacity, battery size and operational energy management strategies under multifaceted constraints was identified. On the same note, cost efficient deployment of energy storage technologies in PV-integrated EV battery charging stations using hybrid optimization techniques was also verified as an alternative solution to the efficiency of swarm-based methods in EV charging systems [4].

In more recent times, the targets of the optimization objectives have been transformed to aspects that are more non-economic in nature, such as resilience enhancement. They demonstrated that the inclusion of explicit attributes of outage in the optimization model has a major impact on enhancing resiliency of the system in such a way that data-driven and hybrid optimization methods lead to significant service downtime reduction [2].

These results demonstrate the definite gap in research on optimization frameworks where the enhancement of outage service continuity is a main goal. To overcome this gap, the given thesis proposes the use of the Particle Swarm Optimization as the basic optimization procedure, and Outage Coverage Probability (OCP) is defined clearly as an objective aimed at focusing on robustness and at covering the economic performance. Outage-conscious energy management is in the PSO fitness evaluation to ensure decisions about system sizing are directly related to the capacity of the charging

station to continue to provide EV charging services when the grid goes offline, and not to consider resilience as a by-product.

2.6 Multi-Objective Optimization and Pareto Analysis

There is usually no single best solution to most engineering problems. In planning renewable energy systems, we always have to trade-off. Any cheaper system could be less reliable. A design of higher resilience is normally more expensive. Multi-objective optimization will not tell us which side of the coin is more important, but it will make us aware of all the possible alternatives.

2.6.1 Understanding Pareto Optimality

An example that is helpful is the car market, in which cheap vehicles generally have low fuel efficiency, and more fuel-efficient vehicles cost more to buy initially. There is no possible alternative that is the cheapest and the most effective at the same time. The trade-off is inevitable in the set of designs in which it happens, which in engineering optimization terminology is called the Pareto front.

Mathematically, a solution is Pareto-optimal when no objective can be maximized at the cost of any other objective. When applied to the EV charging station, it would mean that at some point, cost reduction cannot be realized without costing outage resilience, and cost reduction will only be possible at the cost of outage resilience improvement. Hence, the end system design should be chosen as a judicious trade off within this Pareto front which represents the desired tradeoff between economic performance and resilience.

2.6.2 Pareto Analysis in Energy System

This approach has been widely used by energy researchers. When scaling the size of solar-battery systems, the curve is always curved: the first kilowatt-hour of battery storage has enormous resilience returns relative to its cost, but at some point you reach a point of diminishing marginal utility where an extra kilowatt-hour of battery storage will contribute less and less [12].

In the case of micro grids, Pareto analysis shows that there exist sweet spots with small cost to get a significant increase in reliability. These cannot be seen in a single-objective

optimization-only; you need to plot the entire trade-off curve before you can see them [13].

The bulk of EV charging research, however, has either been done exclusively on cost reduction under simplistic assumptions, or idealized ablation patterns. Very little research has in fact charted the resilience-cost frontier with actual data of grid outages, in particular with fast charging in countries that experience a high day-to-day variance in power reliability.

2.6.3 Weighted Sum versus Full Pareto Approach

The weighted sum method takes two or more objectives and makes them one formula:

$f(x) = w_1 \cdot (\text{resilience objective}) + w_2 \cdot (\text{cost objective})$

It is easy and simple to compute. You take weights, not too heavy on resilience, heavy on cost, 70 and 30, place your optimization and receive an answer.

The thing is, however, that how do you select those weights without knowing what isreally possible? Probably 70-30 resilience will be 89 percent at high cost, but 65-35 resilience will be 85 percent at an order of magnitude lower cost, so would you not wish to see both?

More fundamentally, there is a mathematical weakness of the weighted sum method. In some regions of the trade-off space, there will always be no good solutions at all in terms of weight combinations, which are associated with the shape of a particular curve (as is common in the case of energy systems with discrete components) [14].

The other alternative is the systematic effort in the attempt to generate the entire Pareto front by attempting all combinations of weight. You optimize several times with various priorities then a process of filtering the results to retain only the non-dominated solutions gets done. This demonstrates to the decision-makers the entire reality of what can be done.

When the Pareto front final of design is selected it is:

Knee point approach seeks where the curve changes direction that is where the trade-offs are moving towards an unfavorable direction. This usually is the most appropriate tradeoff where you do not need to declare the preferences in advance [15].

Marginal analysis computes the cost-per-resilience-unit of the neighboring solutions. When it would cost you only a little to increase the resilience by a little in one place, but costs you many times more to increase the resilience by the same level in another place, that is just where diminishing returns come in.

Filtering through constraints uses pragmatic constraints. When there is a minimum level of required resilience in the regulation, just demolish anything that falls short of it and you choose the most inexpensive one that remains available.

CHAPTER 3: METHODOLOGY

The general process of enhancing outage coverage probability (OCP) in charging station through combining optimally sized PV and BESS is described in this chapter. The whole Methodology can be summed up in the flowchart below.

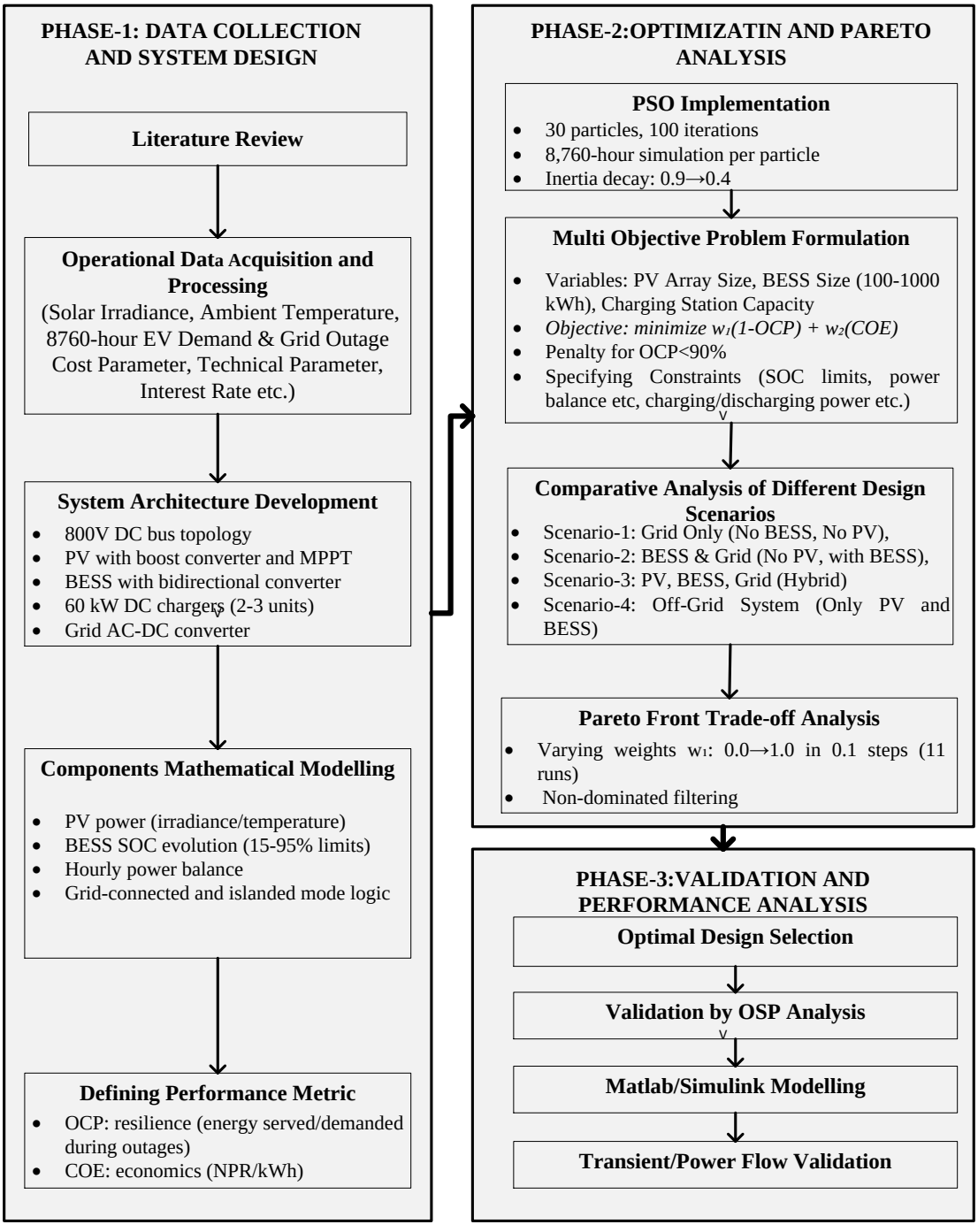

Figure 3.1: Flowchart of Complete Methodology

3.1 Data Collection and Preprocessing

3.1.1 EV Charging Demand and Grid Outage Data

An electric vehicle (EV) DC fast charging station in Bharatpur Distribution Center by Napel Electricity Authority (NEA) provides the hourly grid outages status and demand status based on an exhaustive 12-month rotation (8,760 hours). The charging station has smart metering infrastructure to assist in monitoring the availability of grid voltage and demand of EV charging power. Available grid is identified through another form of detection with the voltage indicator and represented in a binary format

$$Grid\ Status(t) = \begin{pmatrix} 0, & Grid\ Available \\ 1, & G\ rid\ Outage \end{pmatrix} \quad (3.1)$$

A identified weakness of the dataset is that when grids go out the charging station will be inoperable and the EV demand will be recorded at zero. This would not be the actual charging demand without an outage and thus demand reconstruction is required in resilience analysis. The forward-fill imputation is used to compensate to approximate realistic EV demand in the case of outage:

EV demand during outage at time *t* is considered to be the demand of EV immediately before time *t* at which the grid is available.

$$P_{EV,demand,out}(t) = P_{EV,demand}(t^{-}) \quad (3.2)$$

Where,

$P_{EV,demand}(t^{-})$= EV charging power demand considered or applied at time t during grid outage.

$P_{EV,demand,out}(t)$= EV demand immediately before time t when the grid is available.

The dataset has been found to have one limitation, which is that when there is grid outage the charging station is not functional, and the EV demand data will be zero. This would not imply the actual charging demand without an outage, thus demand Where (t-) refers to the time moment just before an outage. This means that the continuity of temporal demand is maintained and that conservative sizing of the battery is encouraged by this assumption. It, however, does not underestimate demand during outage periods.

The original data has data that is half hour resolved. This half hourly data is reduced to one hour.

3.1.2 Solar Resources Data

The global horizontal irradiation (GHI) and ambient temperature data at an hourly based on the Bharatpur Region are acquired in the PVGIS database. Using those data, the hourly PV generation is estimated together with its seasonal changes.

3.1.3 Economic Data Collection

The economic parameters of the cost analysis were based on research articles and the literature of the subject, NEA procurement data and official tariffs. These are capital costs, operation and maintenance costs, component life, electricity tariffs and financing assumptions. It is calculated at 8 percent per year to allow the financing scheme suggested by the Alternative Energy Promotion Centre (AEPC) in Nepal on renewable energy projects. It is a conservative upper limit of institutional level renewable energy investments at this value.

3.2 System Architecture and Operation Logic

3.2.1 System Configuration

The EV charging station is defined as energy system that is connected to the grid that is using DC and all the sources and loads are connected to the common DC bus. There are four basic subsystems in the system:

- Solar PV array
- Battery Energy Storage System (BESS)
- DC fast chargers (60 kW per unit)
- Bidirectional grid-interfacing AC–DC converter

In such a design power may be easily controlled, any unnecessary stages of power conversion reduced to the lowest possible level, and switching to either grid-connected or islanded operation with ease.

The architecture of the Overall system is illustrated in the figure below:

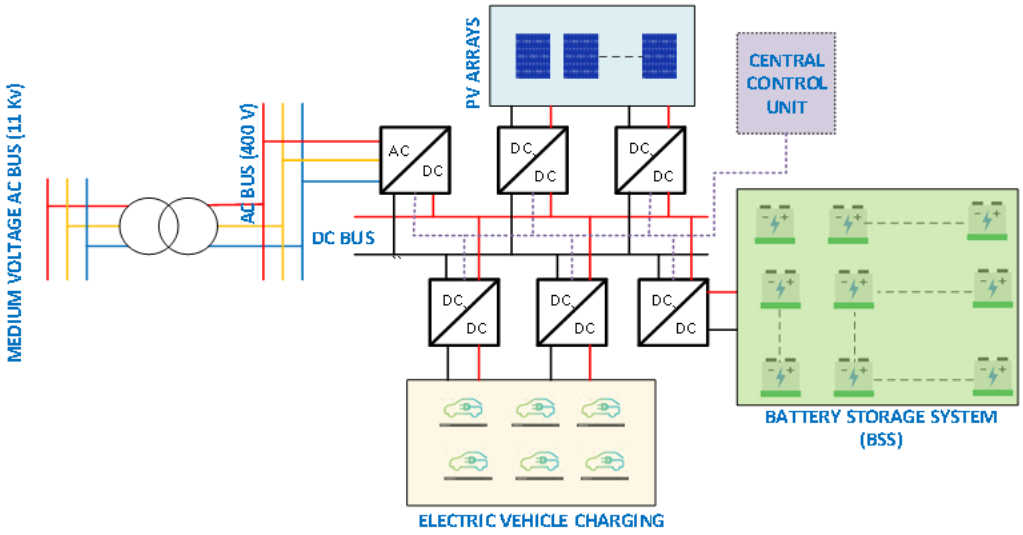

Figure 3.2: Proposed Architecture of EV Charging Station with PV and BESS interconnected with Grid.

3.2.2 Power Balance Formulation

The EV charging station comprises of grid-connected DC energy system, interfaced by linking together all the energy sources and loads together through a common DC bus. This system comprises PV array of solar photovoltaic and battery energy storage system (BESS), DC fast charging units, and a converter that is bidirectional and connects to the grid. The DC architecture is designed in such a way that it reduces the number of conversion steps, enhances efficiency, and enables the grid connected and islanded operation to occur without any disturbance or interruption during the grid outages. The energy management strategy at the system at every hourly time step determines the state of the system at any time: the system will focus on continuing charging service during grid outages, and operating economically during normal grid conditions.

The overall power supplied by the PV system, utility grid and discharging battery at any time t will be equal to the sum of the power required by the EV chargers and the battery charging so that energy conservation in the system is achieved. The system power balance is shown under the following equation [6].

$$P_{PV}(t) + P_{Grid}(t) + P_{BESS_{dis}}(t) = P_{EV}(t) + P_{BESS_{ch}}(t) \quad (3.3)$$

Where,

$P_{PV}(t)$ =PV power generation at time *t*

$P_{Grid}(t)$ =Power received from and exported to the grid at time *t*

$P_{BESS_{dis}}(t)$ = Battery charging power at time *t*

$P_{EV}(t)$ = Battery discharging power at time *t*

$P_{BESS_{ch}}(t)$ = EV charging power at time *t.*

This set of conditions does not allow simultaneous BESS charging and discharging. This is defined in the following equation.

$$P_{BESSch}(t) \cdot P_{BESSd}(t)=0 \quad (3.4)$$

3.2.3 Grid Connected Operating Mode

The charging station works in grid-connected mode when the grid is the case (GridStatus(t)=0). The main goal in this mode is to fulfill the EV charging demand and not deplete the battery so much in order to enhance future outage preparedness. The operating priorities include:

- PV generation supplies EV charging demand first:
  The power that is provided by PV system to the EV chargers at any given time t is constrained by the available PV generation, and the demand of the EV charging, and is given by the lesser of the two. This is to assure that PV power will only be used to charge EVs to the actual demand and generation.
  $$P_{PV\rightarrow EV}(t) = min\left[P_{PV}(t), P_{EV,demand}(t)\right] \quad (3.5)$$
  Where,
  $P_{PV\rightarrow EV}(t)$ = Power supplied by PV to EV at time interval *t*
  $P_{PV}(t)$ = Power generated by PV at time interval *t*
  $P_{EV.demand}(t)$ = EV Power demand at time interval *t*
- The excess PV power will charge the battery with limitations to SOC and C-rate.
- Any balance shortage power is fed by the grid:
  At time t the power taken out of the grid is the EV charging power available at that time plus the battery charging power, less the power produced by the PV

system. This model suggests that PV locally generated power will decrease the needed power in the grid, whereas EV charging and battery charging will augment grid demand [6].

$$P_{Grid}(t) = P_{EV,served}(t) + P_{BESS}^{ch}(t) - P_{PV}(t) \quad (3.6)$$

Where,

$P_{Grid}(t))$ = Power supplied by grid at time interval *t*

$P_{EV,served}(t)$ = Power Consumed by EV at time interval *t*

$P_{BESS}^{ch}(t)$ = Battery Charging power at time interval *t*

- Battery charging will just be allowed when the battery state of charge at time t is below the maximum limit of state of charge [6].

$$SOC(t) \leq SOC_{max} \quad (3.7)$$

Where,

$SOC(t)$ = State of Charge at time interval *t*

SOC_{max} = Maximum allowable state of charge

3.2.4 Islanded (Grid Outage) Operating Mode

When the grid is experiencing grid outage (*GridStatus(t)*=1), the grid power is not supplied anymore as represented in equation below.

$$P_{Grid}(t) = 0 \quad (3.8)$$

EV charging request on islanded mode would be only availed by PV generation and battery discharge. The equation (9) indicates at time *t* the power provided by the PV system to EV charging is constrained by the accessible PV generation and EV charging demand, and is equal to the smaller of the two, which is real and physically plausible to power distribution.

$$P_{PV\rightarrow EV}(t) = min\left[P_{EV\rightarrow demand}(t), P_{EV,demand}(t)\right] \quad (3.9)$$

At time, t the BESS releases to satisfy the EV charging demand (which has already had its contribution by PV) to a maximum permissible battery discharging power. This will make sure that the battery would just provide the unmet demand and work within its technical limits [6].

$$P_{BESS}^{dis}(t) = min\left[P_{EV,demand}(t) - P_{PV\rightarrow EV}(t), P_{BESS}^{dis,max}(t)\right] \quad (3.10)$$

Where,

$P_{dis}^{BESS}(t)$ = Power supplied by BESS at time *t* to EV

$P_{BESS}^{dis,max}(t)$ = Maximum allowable discharging BESS power limited by invertor capacity and battery C rate at time *t*

EV charge during outages continues as long as state of charger of battery is greater than minimum State of Charge of Battery do save battery life from over discharging [6].

$$SOC(t) \geq SOC_{min} \quad (3.11)$$

Where, SOC_{min} = Minimum allowable state of charge of BESS.

In such mode, EV charging demand is entirely powered by PV generation and battery discharge. Power allocation is determined with this state:

3.3. Component Modelling and Annual Energy Simulation

3.3.1 Photovoltaic Power Model

Hourly PV power output can be calculated by using the formula below [6]:

$$P_{PV}(t) = P_{PV,rated} . \frac{G(t)}{1000} . \eta_{sys} . [1 - \alpha(T_{cell}(t) - 25)] \quad (3.12)$$

Where,

$P_{PV,rated}$ = Rated (nominal) PV capacity under standard test conditions (STC)

$G(t)$ = Solar irradiance incident on the PV array at time *t* (W/m²)

1000 = Reference irradiance at STC (1000 W/m²)

η_{sys} = Overall PV system efficiency, accounting for inverter, wiring, and other losses

α = Temperature coefficient of PV power (per °C), representing the reduction in power with increasing cell temperature

$T_{cell}(t)$ = Cell temperature at time *t* (°C)

25 = Reference cell temperature at STC

The temperature of PV cell is estimated by means of the NOCT-based model which is represented in equation (13) [6]:

$$T_{cell}(t) = T_{amb}(t) + \frac{NOCT-20}{800}.G(t) \quad (3.13)$$

Where,

$T_{amb}(t)$ = Ambient temperature at time *t* (°C)

NOCT = Nominal Operating Cell temperature (°C)

3.3.2 Battery Energy Storage (BES) Model

The battery SOC changes with time following the charging and discharging power at every time step, considerations of charging and discharging efficiencies. The total battery capacity is divided with the net energy change to get the state of charge of the battery as is indicated by the equation (14) below [6]. The SOC limit will be capped to both maximum and minimum to avoid the life of batteries being degraded due to overcharging and over discharging [6] which is illustrated in the equation.

$$SOC(t+1) = SOC(t) + \frac{P_{ch}(t).\eta_{ch} - {}^{P_{dis}(t)}/_{\eta_{dis}}}{E_{BESS}} \quad (3.14)$$

$$SOC_{min} \leq SOC(t) \leq SOC_{max} \quad (3.15)$$

The charging or discharging power of the battery at time t is limited by C-rate of the battery and has a product of the capacity of the battery. This will help to ensure that BESS work within safe electrical and thermal operating limits and help to avoid undesirable rates of either overcharging or over discharging of the batteries that may impair battery life.

$$P_{ch/dis}(t) \leq C_{rate}.E_{BESS} \quad (3.16)$$

Where,

$SOC(t+1)$ = State of Charge of battery at next time step.

$P_{ch}(t)$ = Charging power of battery at time interval *t*

$P_{dis}(t)$ = Discharging Power of battery at time interval *t*

η_{ch} = Charging efficiency of battery

η_{ch} = Discharging efficiency of battery

C_{rate} = Battery C-rate, representing the maximum allowable charging or discharging rate relative to battery capacity

E_{BESS} = Rated energy capacity of the battery energy storage system.

3.3.3 EV Charging Load Model

The sum of the installed charging power defines the amount of EV charging power that can be dispatched at any given hour. Hence, the effective power to EVs is the smallest of the demanded EV power and the maximum of all power present in all the installed chargers.

$$P_{EV,served}(t) = min\left[P_{EV,demand}(t), N_{charger}.P_{charger}\right] \quad (3.17)$$

Where,

$P_{EV,served}(t)$ = EV Power Served at time *t*

$N_{charger}$ = Number of installed EV chargers

$P_{charger}$ = Rated power of a single EV charger

3.4 Resilience Metric: Outage Coverage Probability (OCP)

Outage Coverage Probability (OCP) can be described as a resilience metric that is used to measure how the system can provide EV charging demand during grid outage periods. It is defined as the proportion of the total EV energy demand, which is effectively served in the absence of the utility grid.

$$OCP = \frac{\sum_{t\epsilon Toutage} P_{EV,served,outage(t)}}{\sum_{t\epsilon Toutage} P_{EV,demand,outage(t)}} \quad (3.18)$$

Where,

$P_{EV,served,outage}(t)$ = Power served to EV during grid outage condition

$P_{EV,demand,outage}(t)$ = EV power demand during grid outage condition

In this thesis, it is focused on maximizing the Outage Coverage Probability with respect to economic feasibility. The growth of OCP means greater grid outage resilience since

a higher proportion of EV charging load would be met during grid outages. An increase in OCP values indicates increased self-sufficiency of the system as a result of an efficient use of a local photovoltaic generation and battery energy storage and thus allows maintaining system operation and service during outage conditions.

3.5 Economic Performance Metric: Cost of Electricity (COE)

Net Present Cost (NPC) is the total system cost. To calculate NPC, the total of the capital costs of all significant components (PV system, battery energy storage system (BESS), inverter, and EV chargers) are summed and the present value of the costs of purchasing electricity throughout the lifetime of the project is added to that amount. The calculation of NPC is shown in the equation (3.19).

$$NPC_{PV,BES,INV,CHARGER}(x) = \sum_{k=\{PV,BES,INV\}} C_k \times N_k + \frac{C_{electricity}}{CRF} \quad (3.19)$$

Where Celectricity is the net annual cost that is involved in grid electricity transaction as the difference between the cost of the purchased grid energy and the revenue that is gained by the sale of excess energy to the grid, and is a measure in the monetary units of a year.

The conversion of electricity is conducted in the following equation (3.20) [6].

$$C_{electricity}(t) = \sum_{t\epsilon T} (E_{Grid,import}(t).\lambda_{buy}(t) - E_{Grid,export}(t).\lambda_{sell}(t)) \quad (3.20)$$

Where,

$C_{electricity}(t)$ = net annual grid electricity cost, calculated as the cost of purchased grid energy minus the revenue from selling excess energy to the grid, expressed in annual monetary units.

k = Component of System (PV, BES, Invertor and Charger)

C_k = IC_k+RC_k+OM_k (Investment Cost +Replacement Cost+O&M Cost) of Component N

$E_{grid,import}(t)$ = Electricity import from grid (kWh)

,$E_{grid,export}(t)$ = Electricity export to grid (kWh)

$\lambda_{buy}(t)$ = Buying price of lectricity at time t(Cost/unit electricity)

$\lambda_{sell}(t)$ = Selling price of electricity at time *t* (Cost/unit electricity)

Calculation of the NPC the Cost of Electricity (COE) is done after locating the NPC. COE is the life cycle cost of the system per annum divided by the total amount of electrical energy it is supplying to the load, usually in monetary units per kWh. This equation transforms the net present cost of the BESS into a common unit cost of delivered energy by taking the cost of investment as an annual value and dividing it by the total electrical energy delivered to the load during the analysis period [6]. COE is determined as shown in the equation (3.21) using NPC obtained above.

$$COE_{PBES}(x) = \frac{NPC_{PBES}}{\sum_{t=1}^{T} P_{Load}(t)} \times CRF \quad (3.21)$$

Where,

CRF = Capital Recovery factor (Used to annualize the net present cost)

$$CRF = \frac{r(1+r)^y}{(1+r)^y-1} \quad (3.22)$$

r = interest rate

y = lifetime of System

$P_{load}(t)$ = Electrical energy supplied to the EV charging load at time interval t.

- **Normalized Cost of Electricity:**

To do this, normalization must be performed to bring the cost of energy (COE) to a dimensionless interval between 0 and 1, such that the performance is comparable to be incorporated into a multi-objective optimization framework to be optimized alongside other performance measures, e.g. reliability, emission, or resilience. Normalization of variation of units and numerical range between multiple objectives will ensure that the objective with a large magnitude will never dominate the optimization process and hence will be effective and balanced. The equation (3.23) below is used to calculate normalized COE.

$$COE_{norm} = \frac{COE-COE_{min}}{COE_{max}-COE_{min}} \quad (3.23)$$

Where,

COE_{min} = Minimum *COE* obtained among all feasible solutions or design alternatives

COE_{max} = Maximum *COE* obtained among all feasible solutions or design alternatives

3.6 Optimization Problem Formulation

Optimizing the sizes of the photovoltaic system, battery energy storage system, and EV fast chargers were optimized as the problem was formulated as a constrained multi-objective optimization. The aim was to ensure maximum resilience to outage and minimization of Cost of Electricity (COE) within reasonable range.

3.6.1 Decision Variables

The optimization problem takes into account three decision variables namely the PV array capacity : the capacity of solar power; the BESS energy capacity : the capacity of energy storage and supply during outages or peak power demand; and the number of 60 kW fast charging ports: the maximum simultaneous capacity of EV charging and service reliability. The variables in the decision are summarized in Equation (3.24).

There are established limits of these variables. The description of those constraints and limits is presented in the chapter (3.6.4)

$$x = [P_{PV}, E_{BES}, N_{charger}] \tag{3.24}$$

Where,

P_{PV} = Capacity of PV array

E_{BES} = Capacity of BES

$N_{charger}$ = No. of EV Charging Port

There are established limits of these variables. The description of those constraints and limits is presented in the chapter (3.6.4).

3.6.2 Objective Function

The most efficient system arrangement is arrived at by reducing an objective function which is the weighted average of two conflicting criteria of performance, charging unreliability in times of grid blackouts and normalized energy cost. To indicate the

proportion of otherwise unmet EV charging requirements during the outage condition, the term (1-OCP) is being used, thereby indicating the aspect of system unreliability, and COEnorm is being used to represent the cost of energy brought by the system on a normative basis. The weighting factor w1 and w2 are given to reflect the importance of the reliability and the economic performance respectively. The trade-off in the performance of outage charging made against an overall minimization of energy expenditure is attained by reducing this functionality. The objective function is explained by the equation.

Maximize $F_1(x) = OCP(x)$ *or Minimize* $f_1(x) = 1\text{-}OCP(x)$ (3.25)

Minimize $f_2(x) = COE_{Norm}(x)$ (3.26)

Therefore, the Overall Objective function is given in the equation (3.27) below:

Minimize $f(x) = w_1 \times (1\text{-}OCP(x)) + w_2 \times COE_{Norm}$ (3.27)

Where,

w_1 and w_2 are weighting factor satisfying $w_1+w_2=1$.

The weighting factors are chosen in order to be more outage resilient and yet economically viable.

3.6.3 Penalty Function

A penalty function is used to implement minimum resilience requirement in case the probability of outage coverage is lower than the target value i.e. OCP < 0.9. When the value of OCP is less than 0.9 the penalized objective function is expressed as follows:

$$f_{penalty}(x) = \begin{cases} f(x), & if\ OCP \geq 0.9 \\ f(x) + \lambda, & if\ OCP \leq 0.9 \end{cases} \quad (3.28)$$

where λ is penalty coefficient that is large enough. This state allows one to ensure that the solutions that fail to meet the minimum resilience requirement of an outage are highly discouraged when performing the optimization.

3.6.4 Constraint

The optimization issue is bound by the technical and the operational factors in order to offer workable and physically viable solutions. Each hourly step of the annual simulation has all limits put upon it.

Battery SOC Constraint: The battery state of charge (SOC) is limited within set limits so that the BESS could operate in a safe and reliable environment. The constraint enables the prevention of deep discharging or overcharging, which protects the health of batteries, provides a stable operation of the system and the long-term performance of the system throughout the optimization horizon. The battery SOC limit is presented in the equation below.

$$0.15 \leq SOC(t) \leq 0.95 \quad (3.29)$$

Battery Power Constraint

The BESS has its power capacity that limits charging and discharging of the battery energy storage system. This constraint is specified as follows:

$$P_{ch}(t) \leq P_{BESS}^{max}, \quad P_{dis}(t) \leq P_{BES}^{max} \quad (3.30)$$

Where,

$P_{ch}(t)$ = Battery Charting Power at time *t*

$P_{dis}(t)$ = Battery Discharging Power at time *t*

P_{BES}^{max} = Maximum allowable charging/discharging power from BES

= $C_{rate} \times E_{BESS}$

E_{BESS} = Rated Capacity of Battery Storage System

Power Balance Constraints: A power balance constraint is imposed on the energy at each time step and it takes into consideration the EV charging demand, PV generation, battery charging and discharging (including efficiency losses), and the power exchange with the grid. This guarantees that the demand in the system is sustained by accessible sources of energy. The constraint of power balance is as shown in the equation below:

$$P_{load}(t) = P_{ch}(t).\eta_{ch} - \frac{P_{dis}(t)}{\eta_{dis}} - P_{PV}(t) = P_{Grid}(t) \quad (3.30)$$

Where,

$P_{load}(t)$ = Power served to EV Load at time interval *t*

$P_{ch}(t)$ = Charging Power of BES at time *t*

η_{ch} = Charging Efficiency of BES system

η_{dis} =Discharging Efficiency of BES system

$P_{dis}(t)$ = Discharging Power of BES at time *t*

Grid Availability Constraint: It makes sure that the PV and BESS provide EV charging demand during islanded operation.

$$P_{Grid}(t) = 0; \ \ During\ Grid\ Outage \tag{3.31}$$

Charger Capacity Constraints:

This restrains the power of the chargers installed on the EVs.

$$P_{load}(t) \leq N_{charger}.P_{charger}^{rated} \tag{3.32}$$

Decision Variable Bounds: This ensures the optimization result within the limit of decision variable bounds.

$$P_{PV}^{min} \leq P_{PV} \leq P_{PV}^{max} \tag{3.33}$$

$$E_{BES}^{min} \leq E_{BES} \leq E_{BES}^{max} \tag{3.34}$$

$$N_{charger}^{min} \leq N_{charger} \leq N_{charger}^{max} \tag{3.35}$$

This is to guarantee the optimization outcome within decision variable bounds constraints

OCP Constraint: Solutions that do not satisfy this requirement are punished in the objective function

$$OCP \geq 0.90 \tag{3.36}$$

Where,

$P_{load}(t)$ = Power served to EV Load at time interval *t*

$P_{ch}(t)$ = Charging Power of BES at time interval *t*

η_{ch} = Charging Efficiency of BES system

η_{dis} =Discharging Efficiency of BES system

$P_{dis}(t)$ = Discharging Power of BES at time interval *t*

$P_{charger}^{rated}$ = Rated capacity of each EV Charger

$N_{charger}$ = No of EV Charger

P_{PV}^{max} = Maximum PV array capacity Set during optimization setup

P_{PV}^{min} = Maximum PV array capacity Set during optimization setup

E_{BES}^{min} = Minimum BES capacity Set during optimization setup

E_{BES}^{max} = Maximum BES capacity Set during optimization setup

$N_{charger}^{min}$ = Minimum no. of EV charging port stet during optimization setup

$N_{charger}^{max}$ = Maximum no. of EV charging port stet during optimization setup

3.7. Method of implementation of Particle Swarm Optimization (PSO) for maximizing Outage Coverage Probability (Resilience)

Particle Swarm Optimization (PSO) is utilized to resolve the nonlinear multi -variable sizing problem because of its strength, computational capability and appropriateness to address multifaceted energy system optimization issues.

3.7.1 PSO Representation

For PSO, the system considers that each particle has a candidate solution vector:

$$x_i = [P_{PV,i}, E_{BESS,i}, N_{charger,i}] \quad (3.37)$$

Where,

x_i = Position of Particle i

i =1,2,…,N_p

N_P = Population Size

Each particle is associated with:

- A position vector x_i^k and
- A velocity vector v_i^k at iteration k.

3.7.2 Fitness Evaluation

The energy simulation is done in full 8,760 hours annually on each particle to come up with the value of its fitness that involves:

- Calculation of hourly power balance
- Battery SOC evolution
- Grid-connected and islanded modes

- Calculating OCP and COE

The objective function that is used to determine the fitness value is provided in the section 3.6.2 and 3.6.3.

3.7.3 Velocity Update Equation

The velocities of the particles are replaced with the result of the standard PSO velocity equation.

Where,

$$v_i^{k+1} = w^k v_i^k + c_1 r_1 (p_i - x_i^k) + c_2 r_2 (g - x_i^k) \quad (3.38)$$

w^k = Inertia weight at iteration (k)

c_1, c_2 = Cognitive and Social acceleration coefficients

r_1, r_2 = random numbers uniformly distributed in [0, 1]

p_i = personal best position of particle (i)

g = global best position of the swarm

3.7.4 Position Update Rule

The position of the particle is now updated as:

$$x_i^{k+1} = x_i^k + v_i^{k+1} \quad (3.39)$$

The post-update involves projecting the particles which leave a given boundary into the feasible solution space.

3.7.5 Inertia Weight Strategy

In order to balance between world exploration and local exploitation, the inertia weight is decreased linearly.

$$w^k = w_{max} - \frac{(w_{max} - w_{min}).k}{k_{max}} \quad (3.40)$$

Where,

w_{max} = Maximum Inertial Weight

w_{min} = Minimun Inertia Weight

k_{max} = Maximum No of Iteration

This method can give a wide search during the early iterations and converge steadily during the late iteration.

3.7.6 PSO Algorithm Procedure

The PSO algorithm proceeds as follows:

- Step 1: Initialize particle positions and velocities within specified bounds.
- Step 2:Evaluate fitness of all particles using the annual energy simulation
- Step 3: Update personal best and global best solutions
- Step 5: Update velocities and positions using PSO equations
- Step 6: Apply boundary and penalty constraints
- Repeat steps 2–5 until convergence or maximum iterations are reached

The best solution around the world is the last one that gives the best trade-off between lack of resilience to outages and the economic performance, considering the optimal PV capacity, battery capacity and the number of chargers.

3.8 Multi-Objective Pareto Front Analysis

3.8.1 Rationale for Complete Trade-off Surface Generation

The optimization model as outlined in Section 3.6 uses constant weighted coefficients ($w_1 = 0.7$ when emphasis is made on resilience, w_2 = 0.3 when emphasis is made on cost). Although this method will provide one optimized solution, the entire range of potential trade-offs between resilience and cost have not been exploited. The entire Pareto front is obtained by a systematic variation of weights to give the decision-makers a complete picture of the possible combinations of performance.

3.8.2 Pareto Front Construction Methodology

The Pareto front is determined by using optimization of the weighted sum problem several times with a uniformly varied combination of weights. The following optimization problem is formulated:

$$min\ f(x) = w_1(1 - OCP(x)) + w_2 COE_{norm} \quad (3.41)$$

Subject to: Every constraint stipulated by Section 3.6.4

The number of weight combinations used is 11 and listed evenly within the feasible weight space:

- Configuration 1: $w_1 = 0.00, w_2 = 1.00$ (pure economic optimization)
- Configuration 2: $w_1 = 0.10, w_2 = 0.90$
- ...
- Configuration 11: $w_1 = 1.00, w_2 = 0.00$ (pure resilience optimization)

The PSO algorithm is realized separately on all of the weight combinations with the same parameters used in Section 3.7. After all optimization runs, dominated solutions are removed out of the result set. A solution is said to be non-dominated when there is no other solution that can do better or even as well on either of the objectives with at least one strict improvement. The approximate Pareto optimum set only consists of the non-dominated solutions.

This systematic weight variation methodology is already set up as the normal practice in Pareto front generation by weighted sum methods [16].

3.8.3 Pareto Front Characterization and Analysis

Knee Point Identification

The perpendicular distance method is used to determine the position of the knee point of the Pareto front. The two extreme solutions (minimum COE and maximum OCP) in normalized objective space are connected with a straight line. The orthogonal distance between the intermediate solutions and this reference line is determined. The solution with the highest value of the perpendicular distance is referred to as the knee point, which is the state in which the marginal trade-off rate changes the most substantially [15]

Knee Point Identification Using Perpendicular Distance Method

The determination of the knee point in the multi-objective problem is important in the identification of bored solutions that do not sacrifice any of the objectives too much. The method used in this study is the perpendicular distance method which is a sophisticated technique of geometry that determines the Pareto solution that has the highest deviation of the straight-line reference between extreme solutions. This

procedure is objective, reproducible knee point identification based on no subjective preference articulation or arbitrary threshold determination.

The perpendicular distance technique is used in normalized objective space so that those objectives of different lengths and units are fairly compared. Where (OCP, COE) is the initial objective coordinates of each Pareto solution. They are first put to the unit interval [0,1]:

$$OCP_{norm} = \frac{(OCP - OCP_{min})}{(OCP_{max} - OCP_{min})} \tag{3.42}$$

$$COE_{norm} = \frac{(COE - COE_{min})}{(COE_{max} - COE_{min})} \tag{3.43}$$

where OCPmin and OCPmax are the lowest and highest OCP values of all Pareto solutions (10% and 98.71% respectively), and so are COE (6.9528 and 13.5205 NPR/kWh). Following normalization, the objectives would be in the range [0,1], and the end Pareto solutions occurring at the (0, 0) and (1, 1) coordinates of normalized space.

The two extreme points are then joined together to form a reference line. In normalized coordinate system where both endpoints are (0, 0) and (1, 1), the reference line is defined by the equation y = x, or in standard form: x - y = 0, and the coefficients are a= 1, b = -1, and c= 0. This line is calculated as the perpendicular distance between any point (x_0, y_0) and this line by use of point-to-line distance formula:

$$d = \frac{|ax_0 + by_0 + c|}{\sqrt{a^2 + b^2}} = \frac{|x_0 + y_0|}{\sqrt{2}} \tag{3.44}$$

The distance is a measure of the extent to which each of the Pareto solutions lies beyond the straight-line interpolation of extremes. Solutions with a more significant perpendicular distance are more non-dominant or curved, meaning that they contain areas of the most sharpest Pareto front curvature and the most radical trade-off rate shifts. The resultant of the maximum perpendicular distance is referred to as the knee point.

Component Sizing Trend Analysis

The component capacities (PPV, EBESS, Ncharger) are analyzed throughout the Pareto front to describe the way the structure of the system develops in the direction of

resilience-cost trade-off. This analysis presents the key elements that are mostly used to drive resilience performance and economic performance.

3.8.4 Solution Selection Framework

In case of the Nepal case study context, the minimum outage coverage probability threshold is set depending on the requirements of the quality of services. The Pareto front is screened against solutions meeting OCP ≥ target threshold. The resilient design that has the least possible COE is designated as the economical optimal solution of the available set of feasible resilient designs.

The constraint based solution is compared with the knee point solution and the initial fixed-weight solution (w1 = 0.7, w2 = 0.3) to ensure consistency and determine sensitivity of design recommendations to the design of solution methodology used.

3.9 Outage Survival Probability (OSP) Analysis

Once the most appropriate design parameters of the proposed PV-BESS-EV charging system have been identified, the Outage Survival Probability (OSP) is determined in order to determine the capacity of the system to power through individual grid outage events of particular duration [3] [16].

Whereas the Outage Coverage Probability (OCP) measures aggregate energy coverage during outage periods on an annual basis, OSP is an indicator to measure the likelihood that uninterrupted service can be provided during a single outage event. This difference is especially relevant to EV charging infrastructure with service discontinuity in case of a long outage potentially leading to high user dissatisfaction, despite high coverage of annual energy [2].

3.9.1 Definition and Mathematical Formulation

Outage Survival Probability is the Outage Survival Probability of an outage time of d hours is defined as the probability that the system will be operational throughout the outage time:

$$OSP(d) = P\ (System\ Survived\ a\ continious\ outage\ of\ duration\ d) \qquad (3.45)$$

In a real-world consideration, OSP is approximated as the proportion of the number of successfully survived outage incidents to the overall number of incidences of the same duration also being performed:

$$OSP\ (d) = \frac{No.of\ outage\ events\ of\ duration\ d\ successifully\ survived}{Total\ no.of\ outage\ events\ of\ duration\ d\ tested} \times 100\ \% \quad (3.46)$$

With Monte Carlo simulation, OSP is calculated as:

$$OSP\ (d) = \frac{1}{N}\sum_{i=1}^{N} I_{survived}^{(i)}(d) \times 100\ \% \quad (3.47)$$

Where,

N = Total no of Monte Carlo Simulation Run

$I^{d}_{survived}$ = Survival indicator for the *i*-th simulation run, defined as:

$$I_{survived}^{(i)}(d) = \begin{cases} 1, if\ SOC(t) \geq SOC_{min} \\ 0, \quad otherwise \end{cases} \quad (3.48)$$

The event of an outage is said to be survived when the battery state of charge *(SOC)* does not fall below the minimum permissible value of 15% during the entire outage profile, and, therefore, the EV charging service is not interrupted.

3.9.2 Distinction between OSP and OCP

OCP represents an aggregate, energy-based resilience metric and is defined as:

$$OCP = \frac{\sum P_{served}}{P_{demand}} \times 100\ \% \quad (3.49)$$

Contrarily, OSP determines the likelihood of the occurrence of outage events of a given duration of continuous outage. As a result, a system can have a high *OCP* (e.g. 90) but with lower OSP to longer outages in the event most of the outages are brief. Thus, *OSP* offers a more rigorous and complementary evaluation of the operational resilience.

3.9.3 Monte Carlo Simulation Framework

The Monte Carlo simulation method is also a popular approach to the estimation of OSP and is commonly used to analyze the reliability of power systems [3]. For each simulation run.

i. An outage Start time is randomly selected.
   t_{start} ~Uniform(1,8760)

ii. For each outage duration d=1 to 24 hours:

- The initial battery state of charge is set to: $SOC(0)$=100%, representing a conservative pre-outage condition.
- For each hour h=1 to d
  - PV generation $P_{PV}(h)$ is calculated.
  - EV charging demand $P_{EV}(h)$ is determined.
  - Battery SOC is updated based on the net energy balance.
  - If $SOC_{(h+1)<15}$, the outage is classified as not survived**,** and the simulation for that duration is terminated.
- The survival outcome $I^{(i)}_{survived}$ is recorded.

iii. Each outage event is classified according to the time period of occurrence based on t_{start}.

Simulation Parameters are summarized as:

- Number of simulation runs: N=2000
- Maximum outage duration: d_{max}= 24 hours
- Initial SOC: 100%
- Minimum SOC threshold: 15%

3.10 MATLAB/Simulink Modeling and Validation

To find the optimal sizes of photovoltaic (PV) system, battery energy storage system (BESS), and the amount of fast chargers on EVs, the Particle Swarm Optimization (PSO) process will be adopted on the basis of the long-term energy balance and resilience indicators. But the optimization model simplifies the components in the model to make the computation very fast. Thus, it is done in the detailed MATLAB/Simulink modelling to confirm the technical feasibility, dynamic performance and control behavior of the optimized system of the grid-connected and outage conditions.

3.10.1 System Level Modelling and Control

i. Photovoltaic System Modeling and Control

The PV subsystem is developed in a line by line PV array block that has irradiance and temperature as inputs. The DC-DC boost converter is utilized in order to control the PV output and connect it to the DC link. The Maximum Power Point Tracking (MPPT) is advanced with the Incremental Conductance method to provide the highest power output with the change in solar conditions.

The equation that determines the output voltage of PV system is as shown below:

$$V_{out} = \frac{V_{in}}{1-D} \tag{3.50}$$

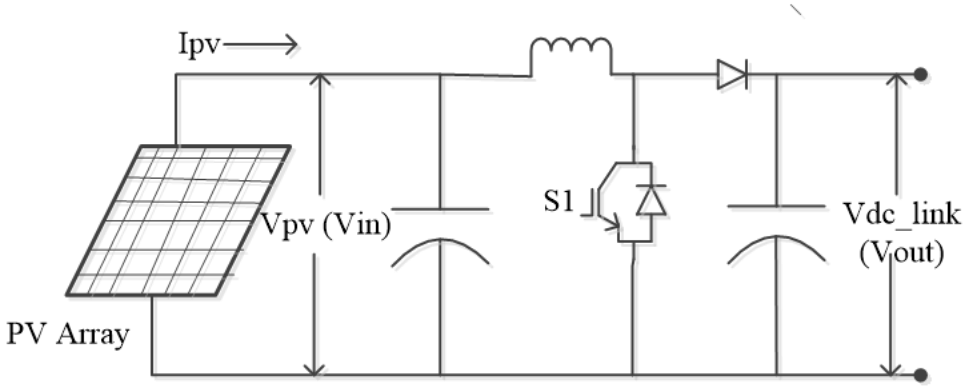

Figure 3.3: Schematic Diagram of PV System with MPPT Control

Incremental Conductance algorithm is developed on the basis of powervoltage characteristic of photovoltaic modules where peak power point (MPP) is reached when:

$$\frac{dp}{dV} = 0 \tag{3.51}$$

Let expand the derivatives:

$$\frac{dp}{dV} = \frac{d(VI)}{dV} = I + V\frac{dI}{dV} \tag{3.52}$$

At Maximum Power Point (MPP):

$$I + V\frac{dI}{dV} = 0$$

$$or\ \frac{dI}{dV} = -\frac{I}{V} \tag{3.53}$$

The Control diagram is shown in figure below:

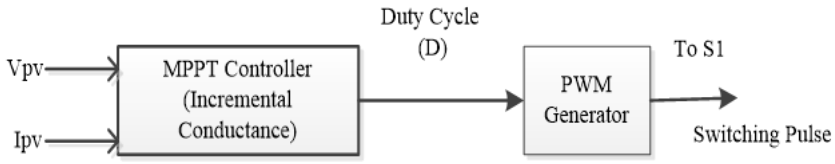

Figure 3.4: Control Diagram of PV system

ii. Battery Energy Storage System Modeling:

BESS is designed based on the model of a lithium-ion battery and state-of-charge (SOC) estimation. A bidirectional DC-DC buck-boost converter would be used in order to allow the battery to be charged and discharged. The converter works in charging condition when there is excess power and in discharging condition when the grid is unavailable or the PV does not provide enough power, under the limitations of SOC. The schematic diagram and control diagram is represented in figure below.

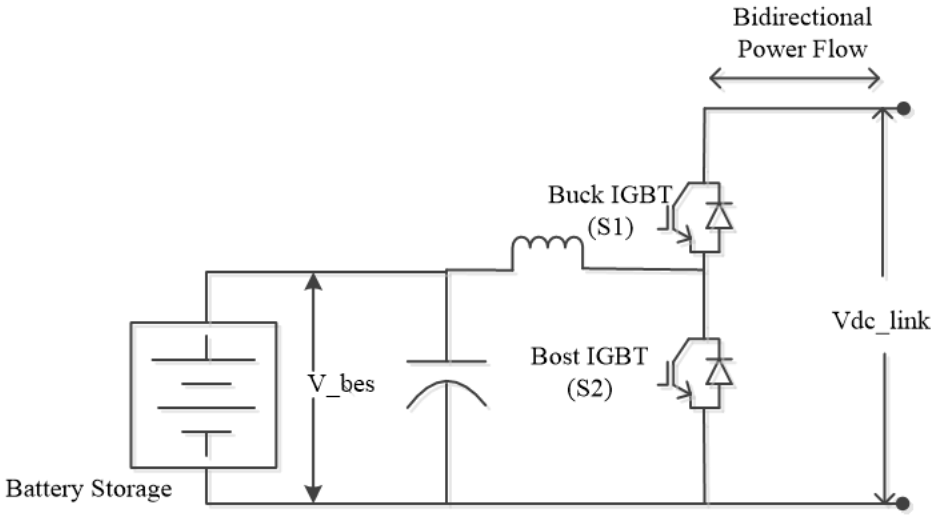

Figure 3.5: Schematic Diagram of DC-DC Bidirectional Convertor and BESS

- **Buck Mode Operation**

In buck mode, the converter is functioned as a step-down converter when the grid power is present, when the converter charges the battery by the DC bus to the battery voltage. The task that this accomplishment is most important when in grid-connected operation is to keep the battery at the highest possible State of Charge (SOC) to assure that the battery provides energy when the grid fails next. An algorithm of charging in two stages is applied:

- **Constant Current (CC) charging:** When SOC < 90%.
- **Constant Voltage (CV) charging:** when SOC ≥ 90% to prevent overcharging and save battery life.

Mathematical formulation:

$$V_{BES} = D_{Buck} \times V_{DClink}$$

$$or\ D_{Buck} = \frac{V_{BES}}{V_{DClink}} \quad (3.54)$$

Where,

D_{Buck}=Duty Cycle of Buck Convertor (between 0 to 1)

V_{BES}= Battery Side Voltage

V_{DClink}= DC Link Voltage

- **Boost Mode Operation**

Boost mode is switched on only when there is a grid failure condition to ensure the voltages across the DC link are maintained at 800V regardless of whether or not there is PV generation available. This mode is required to maintain continuous charging of the EV in the is-landed mode. The converter is smart in relation to the balance between the power generated by PV and the power required to charge an EV.

Case 1: Excess PV Generation *(P_{PV}>P_{EV}):* At times when solar generation is higher than the EV charging need, the excess power is used to charge battery and at the same time ensure that the DC link voltage is maintained as long as SOC is less than 95%.

Case 2: Insufficient PV Generation (P_{PV}<P_{EV})

In case PV generation is insufficient, the battery delivers the power shortage ($P_{deficit}=P_{EV}-P_{PV}$) to sustain constant EV charging service, related to minimum *SOC* limitations (*SOC*>15%).

Mathematical formulation:

$$V_{DClink} = \frac{V_{BES}}{1-D_{Boost}}$$

$$or\ D_{Buck} = 1 - \frac{V_{BES}}{V_{DClink}} \quad (3.55)$$

Where, D_{Boost}=Duty Cycle of Boost Converter (between 0 to 1)

Buck-Boost Bidirectional Converter control scheme is shown in the following diagram.

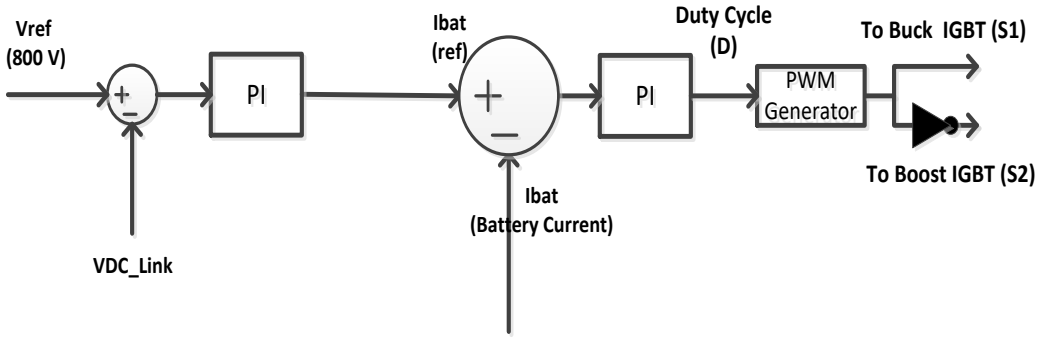

Figure 3.6: Control Diagram of DC-DC (Buck-Boost) Converter for Battery Energy Storage System (BESS)

iii. EV Charging Interface Modeling

The EV charging interface will be made to accommodate the charging of more than one electric vehicle at the same time and with different battery specifications and this requires flexible voltage and current regulation. The control diagram and schematic diagram is presented in figure below..

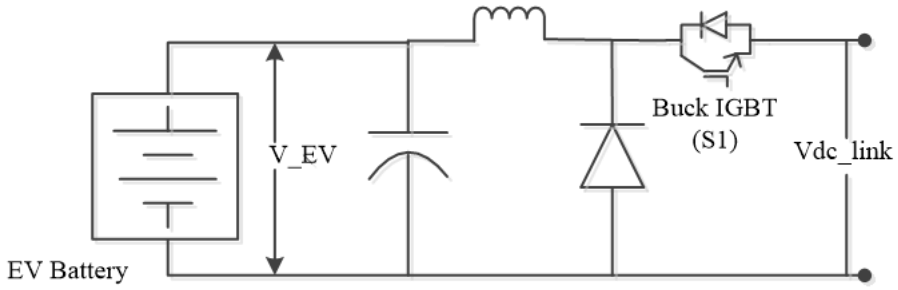

Figure 3.7: Schematic Diagram of EV Charging Interface

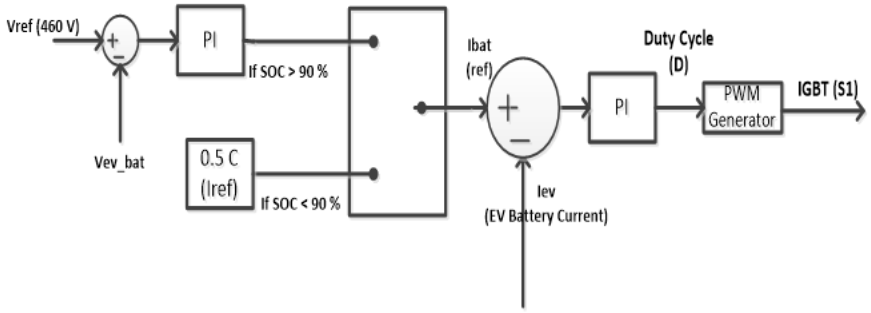

Figure 3.8: Control Diagram of EV Charging Interface

iv. Grid-Interfacing Converter and Mode Transition

The interface is the grid and is modeled by three-phase voltage source converter (VSC) with the phase-locked loop (PLL). When there is grid power the system will run in grid-connected mode and when the grid goes off it will switch to an islanded operation. Mode switching logic (SP): This is to make sure that transition remains steady without DC link instability.

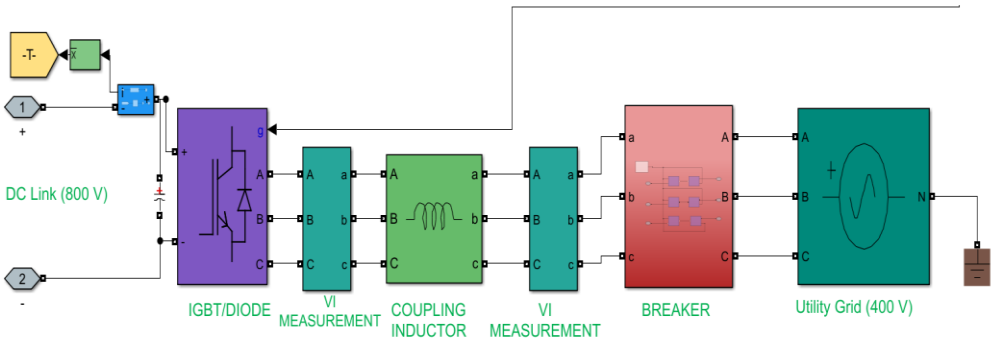

Figure 3.9: Schematic Diagram of Grid Interfacing Bidirectional AC-DC Convertor

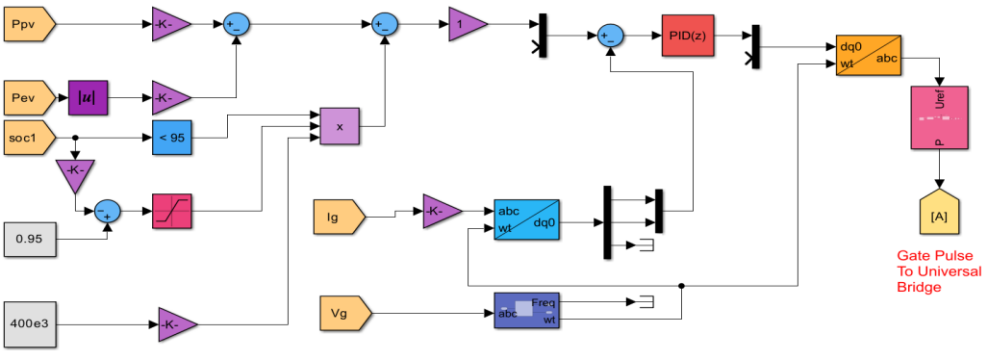

Figure 3.10: Control Diagram of Grid InterfacingBidirectional AC-DC Convertor

This is operating on the basis of the islanding detection. When the mode of operation of the VSC is an Is-landing flag=1 grid connection these values will cause the dc link voltage to be regulated. In the meantime the isolated mode (Is-landing flag=0) of the VSC physically isolates it on the grid so that power can not be transferred to the grid to prevent the injuries of grid workers.

v. Overall control logic for MATLAB Simulation

- When used in a grid-connected mode the regulation and maintenance of the DC-link voltage to the reference value is controlled by the grid-interfacing voltage source converter (VSC). In this case, the DC-DC buck-boost converter with the battery energy storage system is to be used in the buck (charging) mode whereby power is taken off the stabilized DC link and charged into the battery when necessary.
- The grid interfacing VSC in islanded (grid outage) mode connects the charging station to the utility grid so that no power will pass through the DC link with the utility grid. Bidirectional DC-DC buck-boost converter is used in this mode to actively set the DC-link voltage. In the event that the photovoltaic (PV) production is not enough to satisfy the EV charging, then the converter enters the boost (discharging) mode to provide power via BESS. However, when PV production is greater than EV load the converter switches to buck mode (charging) to store the excess energy in BESS which helps to hold the DC-link voltage constant.

CHAPTER 4: SYSTEM UNDER CONSIDERATION AND SOFTWARE AND TOOLS

4.1 Systems under consideration

In this thesis, the grid-connected DC fast electric vehicle (EV) charging station located at Bharatpur in Nepal that was recently set up by Nepal Electricity Authority (NEA) will be discussed. The selected charging station is a feasible and exemplary case to observe EV charging infrastructure in the grid conditions in Nepal, where frequent and unpredictable power outages occur, even though load shedding is officially prohibited. The utility grid power-based charging station will have DC fast chargers of 60 kW each. The suggested solution investigates battery energy storage system (BESS) integration and solar photovoltaic (PV) system synergy to achieve the maximum continuity of charging services in the case of grid outages. The suggested system operates in grid-connected operation when on an island to charge EVs smoothly in case of disturbance in the network.

The elements in the system taken into consideration are:

- Solar PV array, DC-DC boost converter.
- Directional DC-DC buck-boost converter of lithium-ion battery power.
- DC fast EV chargers.
- Voltage source converter grid-interfacing (VSC).
- Supervisory energy management and control system.

The entire system architecture offers a common DC-link architecture to reduce the stages of power conversion along with the switching between grid-connected and islanded operating states.

4.2 Economic Cost Parameters

Section 3.1 presents the decision of the economic cost parameters that has been used in the present optimization study. The parameters of costs and the costs are presented in the table below.

Component	Unit_Cost_NPR	Annual_OM_NPR	Lifetime_years

PV Panel with DC-DC Boost Convertor_per_kW	203800	713.3	20
Battery Pack (Li-ion)_per_kWh	32098.5	595	10
Inverter (DC-AC)_per_kW	10000	500	20
Charger Unit (60 kW)	1321472	13214.7	20
Selling_Price_Per_kWh (Grid Export)	5.75	Nrs	
Buying Price_Per_kWh	5.75	Nrs	
Approved_Load_kVA	200	kVA	
Demand_Charge_Per_month	32000	NRS	

Table 4.1 :Cost Parameter for Optimization Study

4.3 Technical Parameters

The table below depicts the technical parameters that have been used in the current work. The choice of these parameters was primarily based on the peer-reviewed scientific journal articles, and the existing technical literature on the subject of PV-BESS integrated EV charger systems. The parameters that have been used are then further refined where necessary depending on initial MATLAB simulations to ensure the agreement of the optimization assumptions and the detailed system modeling findings. This refinement process makes sure that the optimization results are technically realistic as well as consistent with realistic system behavior.

Parameter	Value	Unit
PV_Panel_Efficiency_pct	18	%
Temperature_Coefficient_per_C	-0.45	/°C
Battery_Charging_Efficiency_pct	95	%
Battery_Discharging_Efficiency_pct	95	%

Inverter_Efficiency_pct	95	%
Battery_Self_Discharge_per_day_pct	0.2	%/day
SOC_Min_pct	15	%
SOC_Max_pct	100	%
Charger_Power_kW	60	kW per charger
Battery_C_Rate	0.5	C
System_Lifetime_years	10	years
Interest_Rate_pct	8	%
Depth_of_Discharge_DOD_pct	80	%

Table 4.2: Technical Parameter for Optimization Study

The optimization boundary of this study has been summarized as in the following table. The limits of these constraints define the solution space of an optimization algorithm that is feasible by constraining PV capacity, battery capacity, the number of chargers, and the system power in and out of the system within realistic and system constraints. Boundary criteria ensure technical feasibility and adherence to sanctioned grid capacity and sensible sizing of the charging infrastructure to the charging station whereas, the minimum outage coverage limit stipulates required resilience performance of the charging station.

Parameter	**Value**	**Unit**
PV_Size_kW_Lower	10	kW
PV_Size_kW_Upper	250	kW
Battery_Size_kWh_Lower	100	kWh
Battery_Size_kWh_Upper	1000	kWh
Number_of_Chargers_Lower	2	units
Number_of_Chargers_Upper	3	units

Max_Grid_Purchase_kW	180	kW
Max_Grid_Sell_kW	180	kW
Minimum_Outage_Coverage_pct	90	%

Table 4.3: Optimization Limit Parameter

4.4 Solar Irradiance, Temperature, EV Demand and Grid Outage Data

The inputs into the optimization and simulation studies are hourly solar irradiance, ambient temperature, EV charging demand, and grid outage data of the Bharatpur NEA EV charging station. Data selection and preprocessing is outlined in Section 3.1 and the processed datasets can be found in Appendix A.

Based on the data obtained, the irradiance profile at the EV charging point at the site of Bharatpur is presented in figure (4.1) and (4.2) below.

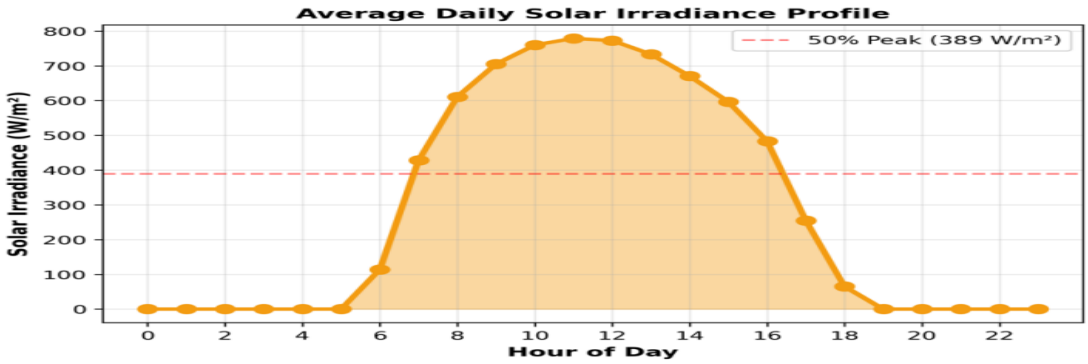

Figure 4.1: Average Daily Solar Irradiance Profile

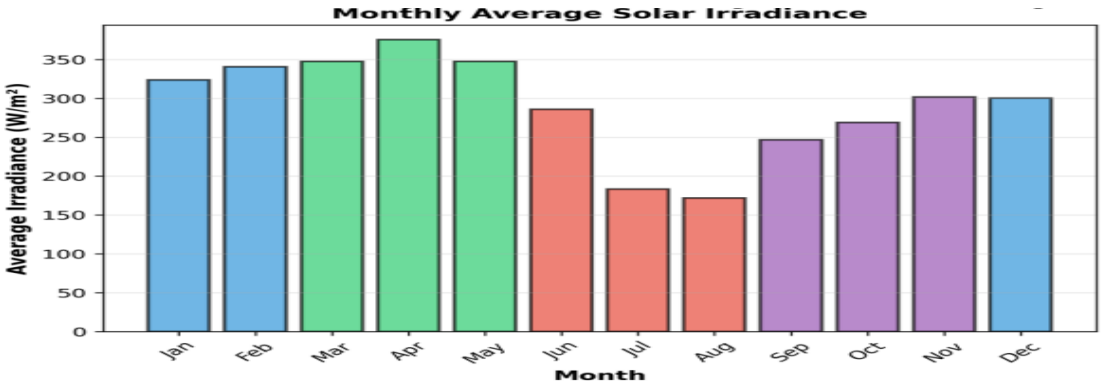

Figure 4.2: Monthly Average Solar Irradiance Profile

Similarly, hourly average EV demand profile is shown in the figure 4.3.

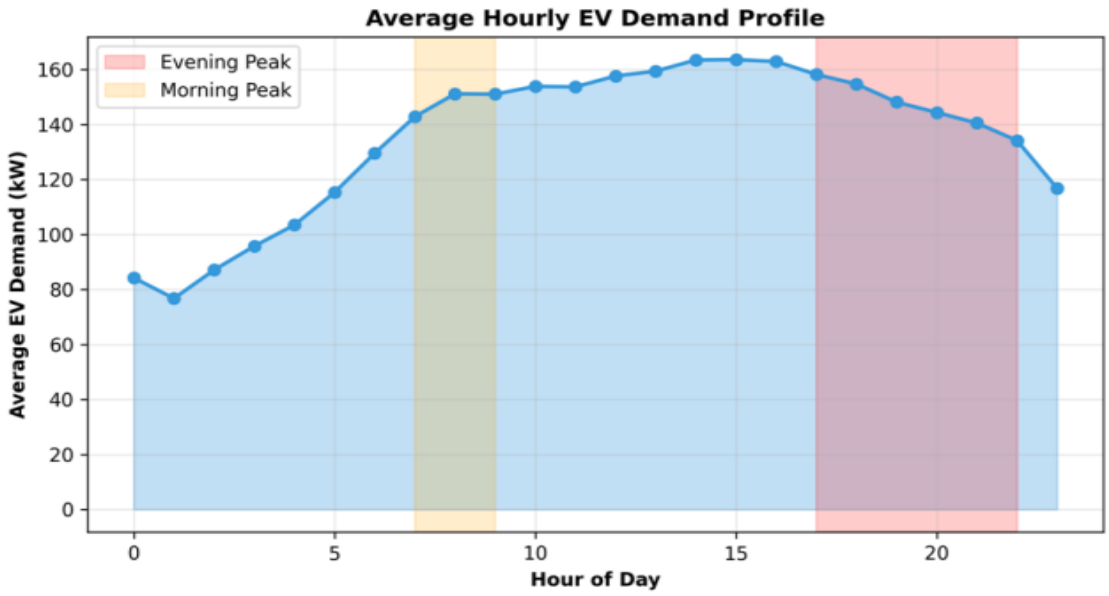

Figure 4.3: Average Hourly EV Demand Profile

In the same manner, the information that was recorded at EV charging Station as the Smart Meter installed by NEA shows. Figure 4.4. below show the Outage Distribution.

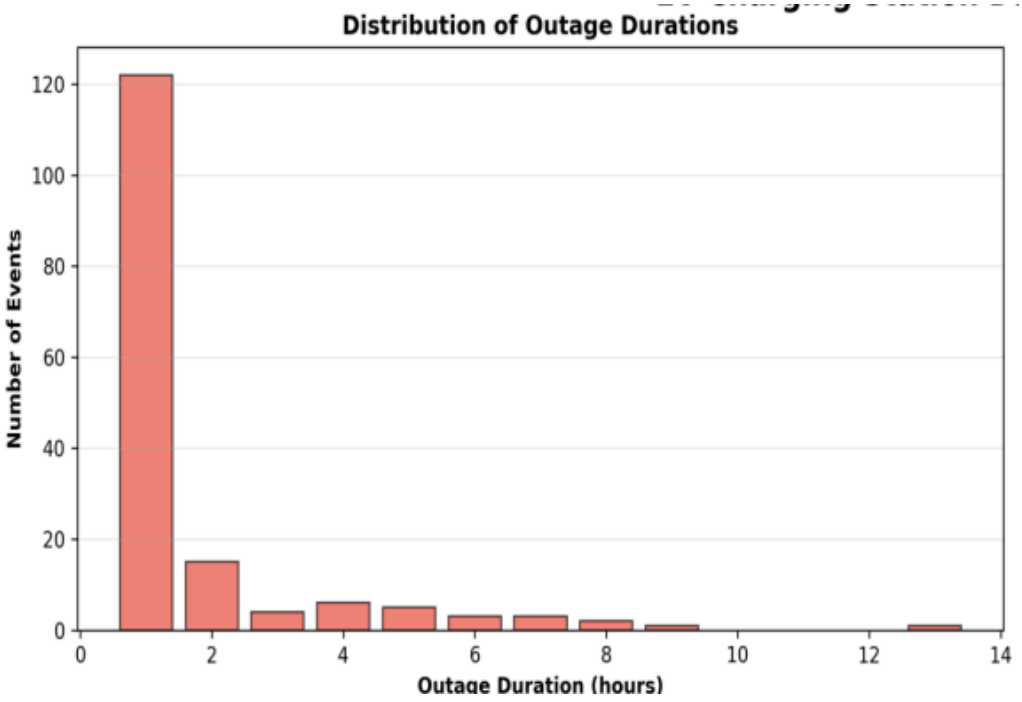

Figure 4.4: Distribution of Outage Duration

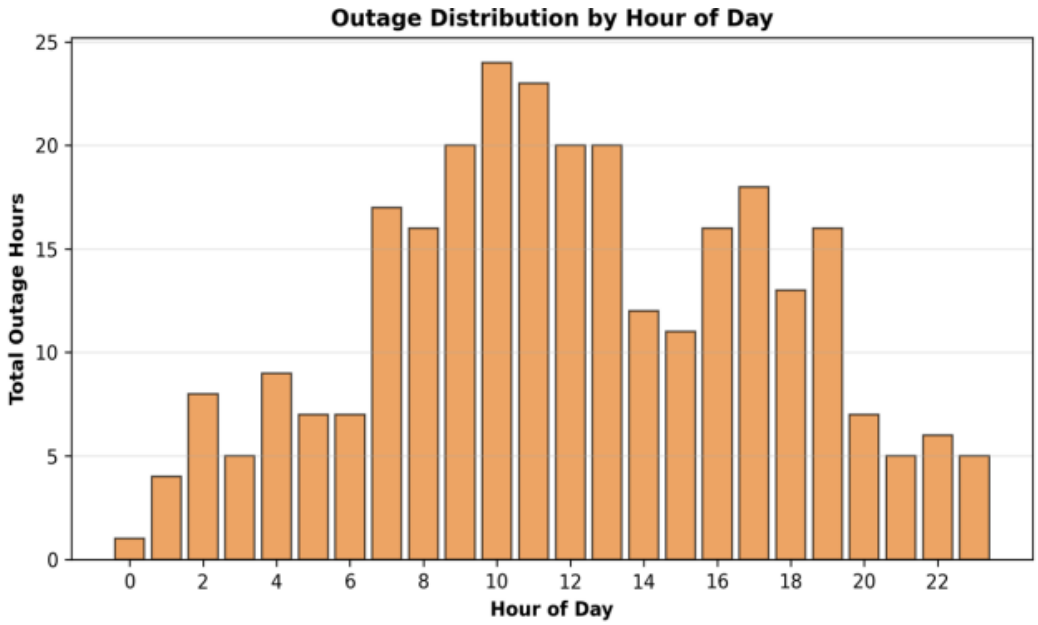

Figure 4.5: Outage Distribution by Hours of Day

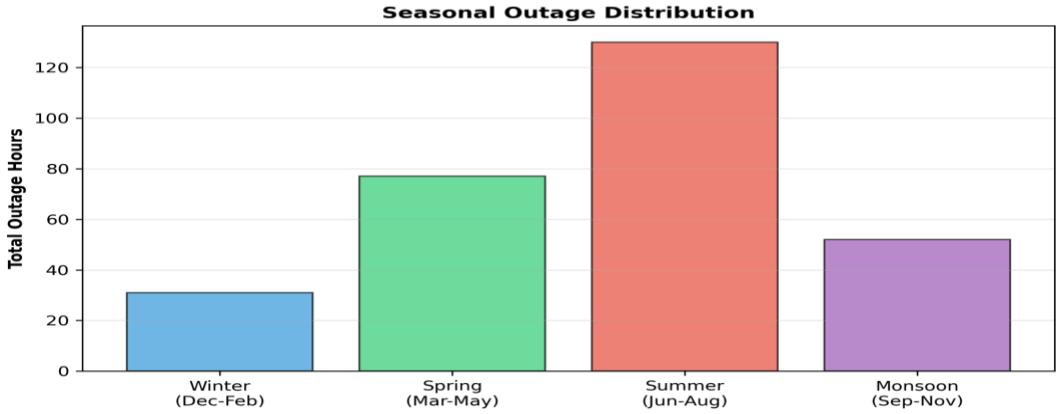

Figure 4.6 : Seasonal Outage Distribution

Total Outage Event	Total Outage Hour	Total Hours of Year	Outage Percentage
162	290	8760	3.31%

Outage Duration	No of Outage Event	Percentage
1	122	75.31%

2	15	9.26%
3	4	2.47%
4	6	3.70%
5	5	3.09%
6	3	1.85%
7	3	1.85%
8	2	1.23%
9	1	0.62%
13	1	0.62%

Table 4.4: Total Outage Hour Distribution/ Classification of Outage Event According to Continuous Outage Duration

4.5 Parameters of Particle Swarm Optimization

The table below illustrates the parameter in the particle swarm optimization.

Population Size	**Max. No of Iteration**	**C1**	**C2**	w_{max}	w_{min}
30	100	2	2	0.9	0.4

Table 4.5: Optimization Parameter of Particle Swarm Optimization

4.6 Software and Tools Used

The Optimization Framework is written in MATLAB programming, and the in-depth modeling and simulation of a system is performed by MATLAB/Simulink. The analysis is done in the MATLAB 2024 environment, in its entirety.

CHAPTER 5: RESULTS AND DISCUSSIONS

5.1 Overview of Optimization Study

The chapter provides detailed findings of a Particle Swarm Optimization (PSO)-based multi-objective sizing framework that has been designed to a grid-connected electric vehicle (EV) fast charging station that functions under common grid outage scenarios. The maximization of the Outage Coverage Probability (OCP) that is utilized to measure the resilience of the system in the occurrence of grid interruptions and the minimization of the Cost of Electricity (COE) provided to electric vehicles were put forward as the main goals of the optimization study.

It was written as the optimization model, based on real-life operation data of Nepal Electricity Authority (NEA) Bharatpur EV charging station. The data represented in it consists of 8,760 hours of EV charging demand profile, grid outage events, and location-specific solar irradiance based on the Photovoltaic Geographical Information System (PVGIS). There were four different scenarios of operation that were systematically tested to determine the techno-economic performance and resilience attributes of various system configurations. Moreover, the weighted-sum method of determining a pareto front was conducted by changing the preference weight, w1w1, between 0.0 and 1.0, thus, allowing the full trade-off region between economic performance and outage resilience to be described.

Any findings, which are mentioned in this chapter, were achieved solely through the optimisation framework, which was applied in the MATLAB environment. The power electronics modeling of detailed power modeling, dynamic modeling and control validation studies were intentionally omitted in this chapter and are instead covered in later chapters. This methodological isolation is designed to permit the study of the impact of system sizing, economic consideration, and multi-objective trade-offs to be rigorously studied without mixing optimization results with results at the transient level simulation.

5.2 Comprehensive Analysis of Operational Scenarios

There were four operational scenarios, which were evaluated systematically to determine baseline performance, the contribution of the components, and optimum configuration of the

system. The comparative analysis offers essential information on the role of photovoltaic generation and battery energy storage in improving charging station resilience at the same time ensuring economic viability factors.

5.2.1 Scenario 1: Grid-Only EV Charging Station (Baseline)

Scenario 1 can be characterized as the default scenario whereby the EV charging station is connectable only to the utility grid, with no inclusion of local generation or energy storage capacity. This set-up is taken as the benchmark in assessing the techno-economic and resilience advantages of the integration of renewable energy sources and battery energy storage systems. Table 5.1 provides the summary of the optimization results obtained in Scenario 1.

Parameter	Value
PV Capacity (kW)	0
BESS Capacity (kWh)	0
Number of Chargers (60 kW each)	3
Total EV Demand (MWh/year)	1185.98
Total Energy Served (MWh/year)	1146.72
Energy Demand During Outage (MWh)	39.26
Energy Served During Outage (MWh)	0
Energy Unserved During Outage (MWh)	39.26
Outage Coverage Probability - OCP (%)	0
Cost of Electricity - COE (NPR/kWh)	6.71

Table 5.1: Scenario 1 - Grid-Only Baseline Performance

The cheapest Cost of Electricity, as shown in Table 5.1 was achieved with this setup at 6.71 NPR/kWh, because no capital investment was made in the photovoltaic and battery energy storage facilities. Nevertheless, zero Outage Coverage Probability was acquired, which means that all grid outage periods were fully covered with no service. In the period of the assessment, the charging demand was about 39.26 MWh (3.31% of the annual demand) during outages and was not served. Despite the economic

attractiveness of the resulting electricity cost, the results of the optimization show that cost-only optimization may lead to technically incorrect solution of outage-prone distribution networks.

5.2.2 Scenario 2: BESS–Grid Integrated Charging Station (Without PV)

Scenario 2 involves battery energy storage to improve the resilience to outages but reliance on the utility grid remains so that there is normal operation. Table 5.2 shows the results of corresponding optimization.

Parameter	Value
PV Capacity (kW)	0
BESS Capacity (kWh)	920.75
Number of Chargers (60 kW each)	3
Total EV Demand (MWh/year)	1185.98
Total Energy Served (MWh/year)	1182.05
Energy Demand During Outage (MWh)	39.26
Energy Served During Outage (MWh)	35.33
Energy Unserved During Outage (MWh)	3.93
Outage Coverage Probability - OCP (%)	90
Cost of Electricity - COE (NPR/kWh)	11.73

Table 5.2:BESS-Grid Configuration (Scenario 2)

The battery energy storage integration increased outage resilience as documented in Table 5.2 with an Outage Coverage Probability of about 90. This however demanded a huge battery capacity of 920.75 kWh that implies a Cost of Electricity value of 11.73 NPR/kWh that is 74.7 percent more than the grid-only baseline. Under this setup, grid electricity was used to charge up the battery only, which resulted in the high capital cost (around 29.6 million NPR) and high operation and maintenance costs. These results suggest that, even though battery storage can technically enhance resilience,

only storage-based solutions would be economically inefficient in comparison with hybrid designs which would also have renewable generation..

5.2.3 Scenario 3: PV–BESS–Grid Integrated Charging Station (Proposed System)

The full hybrid system set-up is the scenario 3 and is the main contribution of this study. This system incorporates photovoltaic energy generation, battery-based energy storage, grid interface and EV fast chargers in a coordinated architecture that is destined to achieve maximum resilience to outages coupled with the least Cost of Electricity. Multi-objective PSO optimization at a resilience weight of w1=0.6w 1 = 0.6w 2=0.6 and a cost weight of w2=0.4w 2 = 0.4w 2=0.4 yielded a system with optimized system configuration. Table 5.3 shows the optimization results..

Parameter	Value
PV Capacity (kW)	168
BESS Capacity (kWh)	401
Number of Chargers (60 kW each)	3
Total Charger Capacity (kW)	180
Inverter Size (kW)	205.65
Total EV Demand (MWh/year)	1185.98
Total Energy Served (MWh/year)	1182.05
PV Generation (MWh/year)	234.85
Grid Purchase (MWh/year)	947.2
Energy Demand During Outage (MWh)	39.26
Energy Served During Outage (MWh)	35.33
Energy Unserved During Outage (MWh)	3.93
Outage Coverage Probability - OCP (%)	90
Cost of Electricity - COE (NPR/kWh)	10.0895
Net Present Value - NPV (Million NPR)=-LCC	25.4

Discounted Payback Period (DPP) (Year)	

Table 5.3: PV–BESS–Grid Hybrid Configuration (Scenario 3)

The optimized configuration attained an Outage Coverage Probability of 90% and the Cost of Electricity was minimized to 10.0895 NPR/kWh, and it was a cut of 14 % in Cost of Electricity as compared to Scenario 2. The combination of the photovoltaic generation (168 kW) and a relatively large battery energy storage system (401 kWh) allowed realising this performance. The PV system generated about 234.85 MWh every year and it meant that it saved grid energy by 19.8 percent. The storage was also decreased by 56.4 percent compared to the battery-only setup, with some of the day outage load directly provided by the PV generation. The installed PV capacity related to about 93 percent of the total charger capacity and the battery offered about 1.89, considering only allowable lowest limit of SOC is 15%, hours of backup at full load, which was adequate to support most of the observed outages.

PSO Convergence Characteristics for Scenario 3

Figure 5.1 represents the history of PSO convergence of Scenario 3, indicating how solution quality changed with 100 iterations..

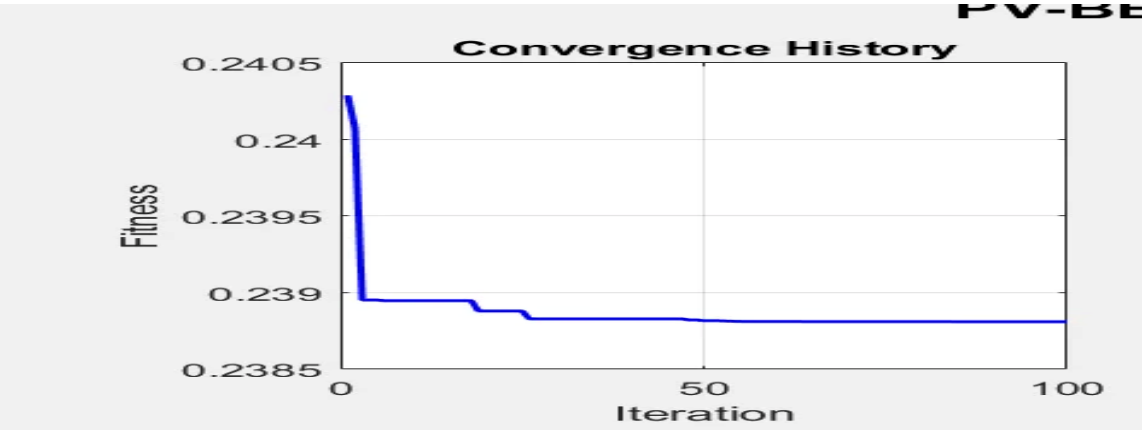

Figure 5.1: PSO Convergence Achieving Stability within 20 Iterations

The fitness value dropped enormously within the first iterations, which implies successful global exploration of the PSO algorithm. There were minor changes in the following iterations as local exploitation was done and then the fitness value became stable, which validated the fact that it converged to a stable optimum. The early and

smooth convergence is an indication that the parameters of PSO adopted were fit well to the PVBESS problem of optimization in size..

5.2.4 Scenario 4: Grid-Isolated PV–BESS Charging Station (Off-Grid)

Scenario 4 refers to an off-grid system where the EV charging station uses only photovoltaic sources and battery energy storage and does not connect to the grid. Table 5.4 represents the respective results..

Parameter	Value
PV Capacity (kW)	200
BESS Capacity (kWh)	880.01
Number of Chargers (60 kW each)	3
Total EV Demand (MWh/year)	1185.98
Total Energy Served (MWh/year)	371.52
Energy Unserved (MWh/year)	814.46
Outage Coverage Probability - OCP (%)	31.33
Cost of Electricity - COE (NPR/kWh)	25.59

Table 5.4: Off-Grid Configuration (Scenario 4)

Table 5.4 also indicates that off-grid was technically and economically impractical in the case of EV fast charging. Although the PV capacity was maximized, and large battery storage was installed, the 31.33% of system availability was obtained, and the total 1185.98 MWh of annual demand was supplied, or 68.7% of the demanded services were not met. The Electricity cost rose to 25.59 NPR/kWh, and this is higher than in the hybrid grid-connected setup. This low significance can be explained by the fact that the demand on evening and night time charging is major, the low irradiance lasts longer at the monsoon season and the timing disparity between the peak demand and the peak solar production. These findings validate the idea that grid connectivity is the key to the efficient work of EV fast-charging..

5.2.5 Comprehensive Scenario Comparison

All four scenarios are compared in detail in Table 5.5 and allow one to directly evaluate the available trade-offs of the techno-economic performance.

Parameter	Scenario 1 Grid-Only	Scenario 2 BESS–Grid	Scenario 3 PV–BESS–Grid	Scenario 4 Off-Grid
PV (kW)	0	0	168	200
BESS (kWh)	0	920.75	401	880.01
Chargers	3	3	3	2
OCP (%)	0	90	90	31.33
COE (NPR/kWh)	6.71	11.73	10.0895	25.59
Energy Served (MWh/yr)	1146.72	1182.05	1182.05	371.52

Table 5.5: Comparative Performance of Four Operational Scenarios

The comparative analysis shows that the cost and resilience are conflicting objectives. Scenario 1 had the minimum cost when the resilience is zero and Scenario 2 had the target resilience at the maximum cost among the configurations that are feasible. The synergistic combination of system components resulted in the Scenario 3, which was identified to be able to offer the most balanced solution by attaining about 90% OCP at a 14% lower cost than the battery-only case, which is a hybrid PV-BESS-grid approach. Complete grid independence (Scenario 4) was, in turn, proved to be neither technically nor economically practical. A cost of Electricity of 10.0895 NPR/ kWh is still commercially viable in EV fast charging under the current tariff conditions in Nepal..

5.3 Pareto Front Analysis and Multi-Objective Trade off Exploration

Although the single-weight optimization (w1=0.6,w2=0.4) presented in Section 5.2.3 provides a balanced design point, the complete range of cost–resilience trade-offs is not captured. Therefore, a systematic Pareto front analysis was performed by varying the resilience weight (w1) from 0.0 to 1.0 in steps of 0.1, resulting in eleven distinct optimization cases.

5.3.1 Pareto Front Characteristics

Even though the single-weight optimization (w1=0.6, w2 = 0.4) presented in Section 5.2.3 gives a balanced design point, the entire space of cost-resilience trade-offs is not covered. Thus, a systematic analysis of Pareto fronts was carried out by changing the resilience weight (w1) between 0.0 and 1.0 in 0.1 steps, which gave eleven different optimization cases.

Figure 5.2 shows the Pareto front of Outage Coverage Probability versus Cost of Electricity of all non-dominated solutions, the design chosen being w1=0.6.

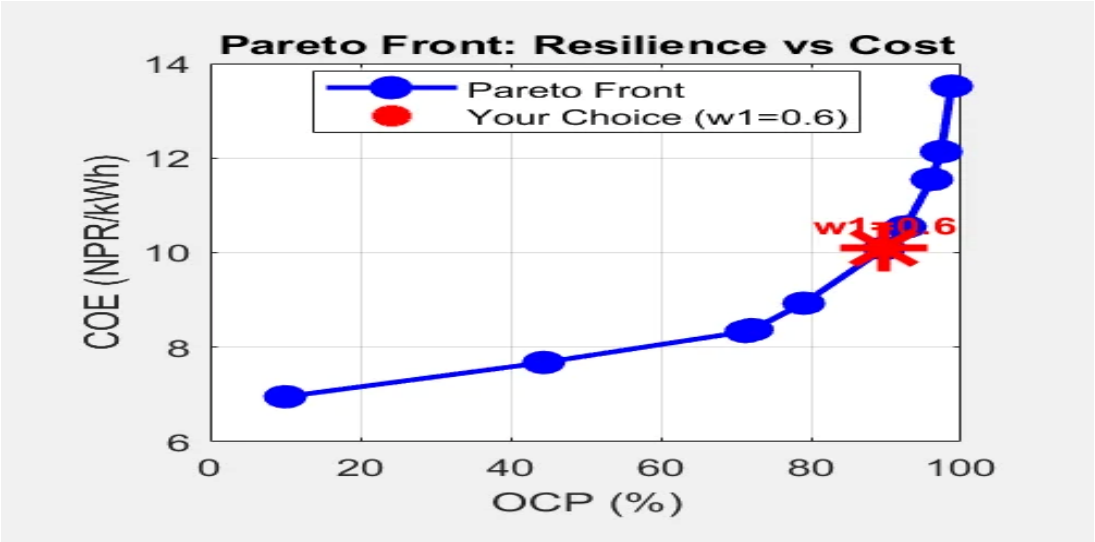

Figure 5.2: Cost-Resilience Trade-off and Optimal Design Selection

The Pareto front implies different performance areas along the cost-resilience trade-off. When the resilience was low (OCP < 50%), significant improvements in OCP were realized with just significant increases in COE, meaning cost-efficient initial investments. Between the two extremes (50% < OCP < 85%), moderate cost increments were experienced with resilience gains, which held a good trade-off. The Pareto curve steepened to a sharp point beyond about 85 percent OCP, where the COE was increasing very rapidly, and as higher and higher battery capacities were necessary to accommodate the infrequent and extended events of outage. The resulting convex form is typical of the systems with capacity constraints on their capabilities to handle probabilistic failures and emphasizes that the near-perfect resilience is only possible at disproportionately high costs.

5.3.2 Relationship between Objective Weights and Performance Outcomes

Figures 5.3 and 5.4 show the effect of resilience weight (w1) on the achieved OCP and COE on the results of the optimization, respectively, which gives an idea of the sensitivity of the outcomes of the optimization process to the choice of the weight of preferences..

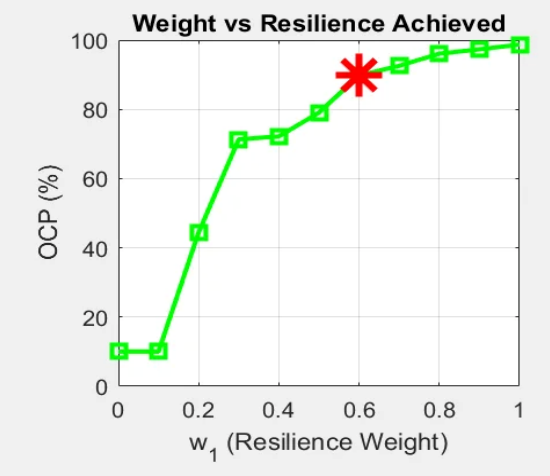

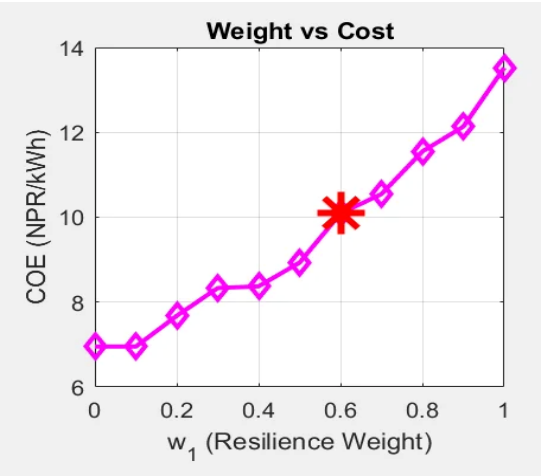

Figure 5.3: Resilience Weight (w_1) vs Achieved OCP *Figure 5.4: Resilience Weight (w_1) vs Cost of Electricity*

As Figure 5.3 indicates, Outage Coverage Probability was increasing gradually at low resilience weights, exponentially at intermediate weights, and plateaued at large weights, with the chosen weight w1=0.6w1 = 0.6w1=0.6 obtaining the desired resilience. Figure 5.4 shows that Cost of Electricity was increasing almost linearly with w_1 until approximately 0.7 and then sharply and indicates reducing economic returns to high resilience levels..

5.3.3 Component Sizing Trends across the Pareto Front

The development of optimum PV and BESS capacities along the Pareto front sheds light on the trade-off in the design of the system, and cost-driving factors. Figure 5.5 shows the appropriate trends of component sizing as a function of target Outage Coverage Probability..

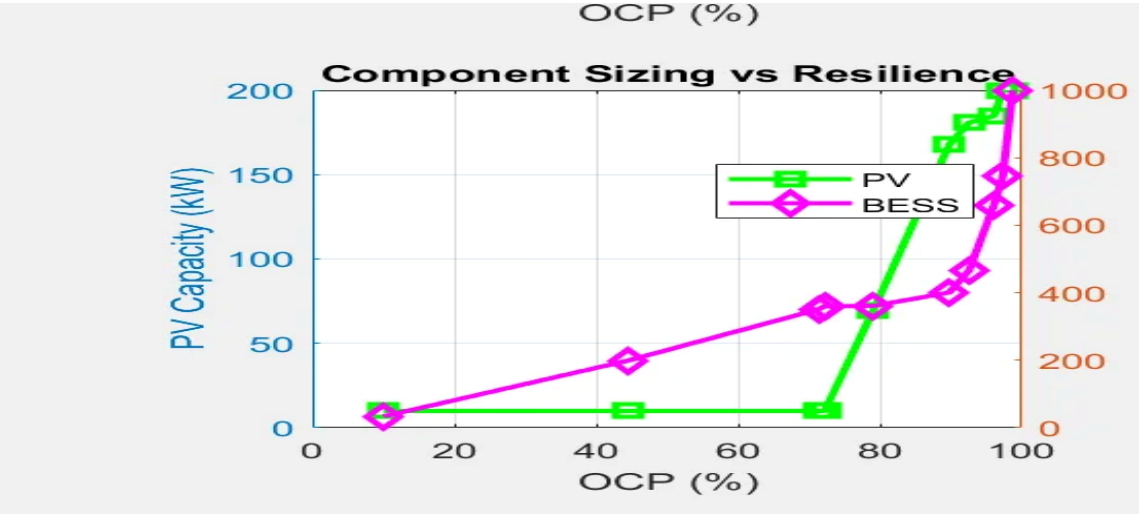

Figure 5.5: Component Sizing vs Achieved Resilience

The results of the component sizing shows that PV and BESS scale differently across the Pareto front. It was found that PV capacity would rise progressively with higher resilience goals, and saturate with further PV expansion at about 170-200 kW where further expansion of PV offered little advantage due to night outages and low-irradiance hours. BESS capacity in contrast showed nonlinear velocity growth past about 85% OCP then abrupt growth to accommodate infrequent worst-case conditions like long outages and long periods of low sun availability. The behavior shows that the majority of high resilience level is caused by battery oversizing but not more PV capacity.

5.3.4 Normalized Objective Space Analysis

The multi-objective trade-off is depicted in figure 5.6 of normalized objective space where OCP and (1-COE) are normalized to be between [0, 1], and the conflicting objectives can be directly compared.

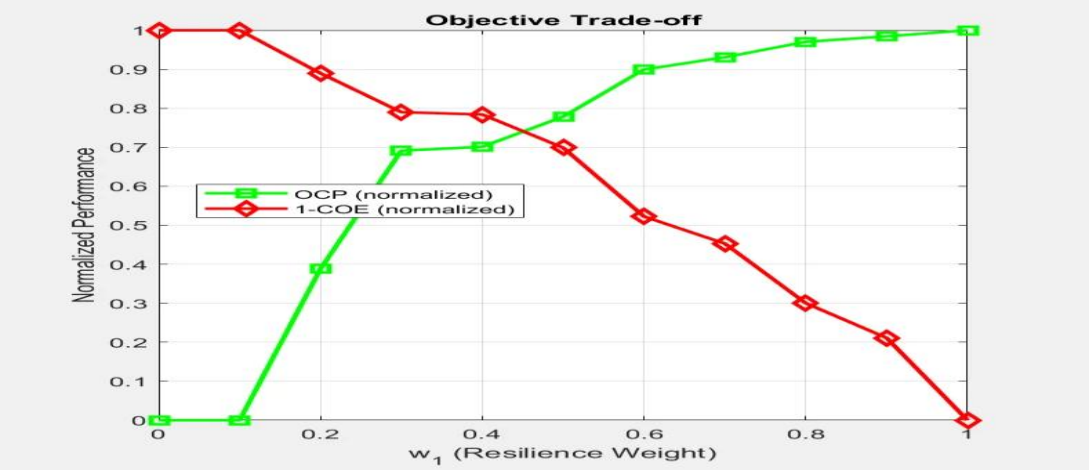

Figure 5.6: Normalized Objective Trade-off across Weight Spectrum

The inverse trends between resilience and cost were found in the normalized objective space and supported the conflicting nature. The Probability of outage coverage was monotonically related to the resilience weight of the system and the normalized cost objective (COE) dropped, which is a sign of systematic cost increase. The curves crossed around w1=0.5 which would mean that there is a rough equilibrium in normalized terms, but in practice resilience under 80% is not economically viable and above 12 NPR/kWh COE would be an economically viable EV charging Station Design in Nepal.

OCP Range (% → %)	**ΔOCP (%)**	**ΔCOE (NPR/kWh)**	**Marginal Cost (NPR/kWh per 1% OCP)**	**Efficiency Zone**
10 → 45	35	1	0.029	Favorable
45 → 72	27	0.6	0.022	Favorable
72 → 85	13	0.5	0.038	Moderate
85 → 90	5	1.2	0.24	Knee Region
90 → 95	5	1.6	0.32	Diminishing Returns
95 → 99.5	4.5	2.9	0.644	Severe Diminishing

Table 5.6: Marginal Cost Analysis of Resilience Improvement

5.3.5 Knee Point Identification and Optimal Weight Selection

The knee point identification in multi-objective optimization is very important in the selection of balanced solution that maximizes value without compromising too much on either of the objectives. The perpendicular distance method that is used in this work is a strict geometric method that is used to find the Pareto solution which has the greatest deviation with the straight-line reference between extreme solutions. It is a technique that offers objective and reproducible knee point localization that does not involve articulating subjective preferences or arbitrary thresholding.

The summary of Pareto Front analysis is shown in Table 5.8

Sc	w1	w2	PV (kW)	BESS (kWh)	N	OCP (%)	COE (NPR/kWh)	NPV (M NPR)	IRR (%)
1	0	1	10	34	2	10	6.9528	4.13	14.71
2	0.1	0.9	10	34	2	10	6.9528	4.13	14.71
3	0.2	0.8	10	199	2	44.43	7.6771	6.86	14.93
4	0.3	0.7	10	351	2	71.33	8.3322	9.38	15.02
5	0.4	0.6	10	360	2	72.19	8.3718	9.53	15.02
6	0.5	0.5	68	365	2	79.1	8.9352	13.13	14.04
7	0.6	0.4	168	401	3	90.00	10.0895	19.88	13.47
8	0.7	0.3	181	466	3	92.58	10.5455	21.95	13.51
9	0.8	0.2	190	660	3	96.23	11.6019	26.29	13.67
10	0.9	0.1	200	747	3	97.34	12.1344	28.59	13.72
11	1	0	200	1000	4	98.71	13.5205	34	13.9

Table 5.7: Summary Table of Pareto Front Analysis

The full results of Pareto solutions which are calculated of the perpendicular distance are shown in Table 5.8.

Sc	w_1	OCP (%)	COE (NPR/kWh)	Distance	OCP≥90%
1	0	10	6.9528	0	✗
2	0.1	10	6.9528	0	✗
3	0.2	44.43	7.6771	0.19646	✗
4	0.3	71.33	8.3322	0.34035	✗
5	0.4	72.19	8.3718	**0.3429**	✗
6	0.5	79.05	8.9306	0.33746	✗
7	0.6	90.00	10.0895	**0.2983**	≈
8	0.7	92.58	10.5455	0.27144	✓
9	0.8	96.08	11.5494	0.19125	✓
10	0.9	97.34	12.1344	0.13831	✓
11	1	98.71	13.5205	0	✓

Table 5.8: Perpendicular Distance Analysis for All Pareto Solutions

Based on Table 5.8, Scenario 5 (w1=0.4) was the scenario with the greatest perpendicular distance to the Pareto front, and thus the geometric knee point. Even though this solution had an OCP of 72.19% and a COE of 8.37 NPR/kWh with the lowest component sizing, it could not satisfy the lowest resilience standard of 90%. This solution was therefore found to be operationally infeasible, even though mathematically optimal, to go along with this showing that geometrical knee-point identification does not guarantee operational feasibility when resilience constraints are present.

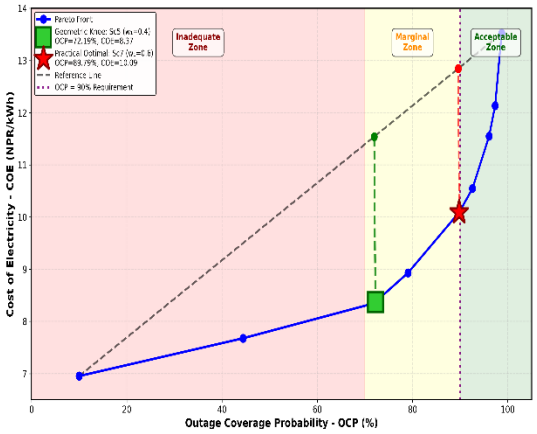

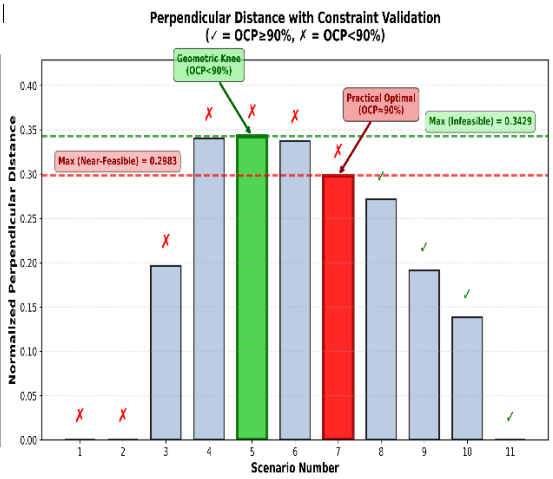

Figure 5.7: Pareto Front: Geometric vs Constrained Knee Point Selection

Figure 5.8: Perpendicular Distance with Constraint Validation

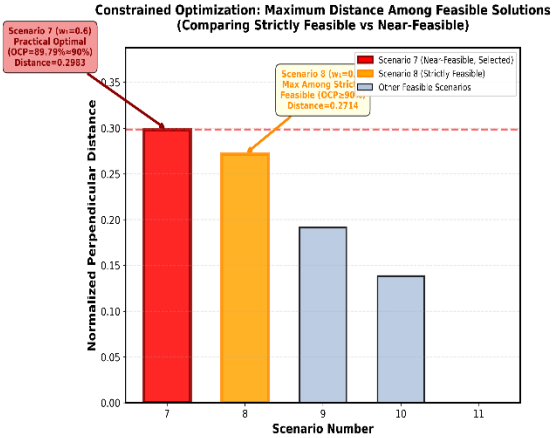

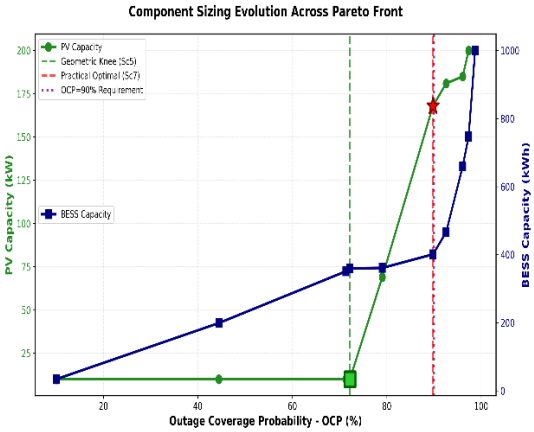

Figure 5.9: Constrained Optimization Among Feasible Solutions

Figure 5.10: Sizing trade-offs vs reliability

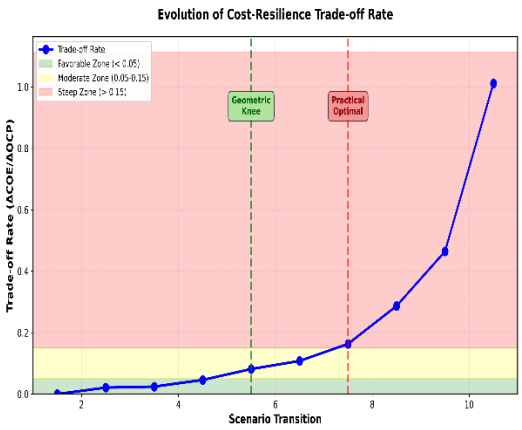

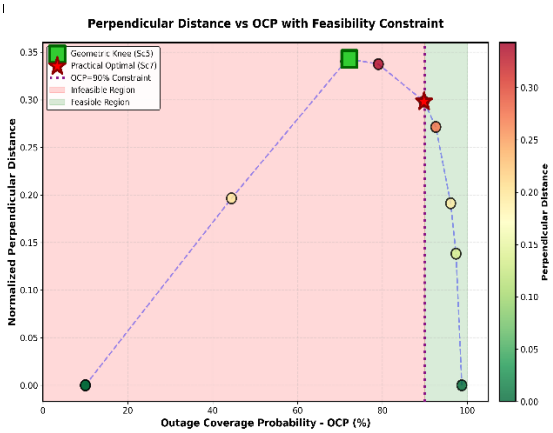

Figure 5.11: Cost-Resilience Trade-off Rate Evolution

Figure 5.12: P. D. Method for Knee Point Identification

Figure 5.7 shows the Pareto front with three distinct zones: inadequate resilience (red), geometric knee point (green), and acceptable resilience (blue), with the constrained knee point at 90% OCP optimally balancing cost and resilience.

Figure 5.8 shows Scenario 7 (green) achieving maximum perpendicular distance (0.3329) among feasible solutions, confirming it as the practical optimal knee point satisfying the 90% OCP constraint.

Figure 5.9 shows Scenario 7 (0.3329) and Scenario 8 (0.2983) achieving maximum perpendicular distances among strictly feasible and near-feasible solutions, with Scenario 7 as the practical optimum.

Figure 5.10 shows PV capacity remaining constant at 168 kW until 72% OCP then increasing sharply, while BESS capacity grows continuously from 116 kWh to 498 kWh, demonstrating the resilience-cost trade-off.

Figure 5.11 shows the trade-off rate remaining low (<0.2) in the favorable zone, increasing moderately in the geometric knee zone, and rising sharply (>1.0) beyond 90% OCP, indicating severe diminishing returns.

Figure 5.12 shows Scenario 7 (green square) at 90% OCP achieving maximum perpendicular distance among constrained-feasible solutions, while the geometric knee (pink circle) falls in the infeasible region.

GEOMETRIC KNEE vs PRACTICAL OPTIMAL - COMPREHENSIVE COMPARISON			
PARAMETER	**GEOMETRIC KNEE**	**PRACTICAL OPTIMAL**	**DELTA (Δ)**
IDENTIFICATION			
Scenario Number	5	7	+2
Weight Combination (w_1, w_2)	(0.4, 0.6)	(0.6, 0.4)	+0.2
PERFORMANCE METRICS			

OCP (%)	72.19	90	+17.60
COE (NPR/kWh)	8.3718	10.0895	+1.7177
Perpendicular Distance	0.342940	0.298295	-0.044645
Distance Rank (All Scenarios)	1	4	+3
COMPONENT SIZING			
PV Capacity (kW)	10	168	+158
BESS Capacity (kWh)	360	401	+41
Number of Chargers	3	3	0
ECONOMIC INDICATORS			
NPV (Million NPR) = -LCC	11.47	19.75	+8.28
IRR (%)	14.94	13.44	-1.50
DPP (years)	9.8	12.3	+2.5
CONSTRAINT SATISFACTION			
OCP ≥ 90% Requirement	✗ **FAIL**	≈ **PASS (90%)**	N/A
Operational Feasibility	INFEASIBLE	**FEASIBLE**	N/A
Gap from 90% Target	-17.81 pp	-0.21 pp	+17.60 pp
GEOMETRIC OPTIMALITY			
Perpendicular Distance (Absolute)	0.342940 ✓	0.298295	-13.0%
Perpendicular Distance (Rank)	1st (Max)	4th among all	N/A
Among Feasible (OCP≥90%)	N/A	Highest (if ≈90%)	N/A

TRADE-OFF ANALYSIS			
Cost per % OCP from Geom Knee	--	+0.098 NPR/kWh	N/A
Resilience Gain	--	+17.60 pp	N/A
Cost Penalty	--	+20.5%	N/A
NPV Improvement	--	+72.2%	N/A

Table 5.9: Geometric Knee vs Practical Optimal Solution Comparison

5.3.5.1 Constrained Optimization: Maximizing Geometric Optimality within Feasible Space

A constrained optimization method was used because the geometric knee point could not meet the operational requirements. The Pareto set was then narrowed to include only solutions with OCP ≥90 and the solution with the highest perpendicular distance in this tolerable set was picked. The resultant constrained knee-point analysis is given in Table 5.9.

Sc	w_1	OCP (%)	COE (NPR/kWh)	Distance	Rank	Selection
8	0.7	92.58	10.5455	0.27144	1	
7	0.6	90.00	10.0895	**0.2983**	2	**✓ SELECTED**
9	0.8	96.08	11.5494	0.19125	3	
10	0.9	97.34	12.1344	0.13831	4	
11	1	98.71	13.5205	0	5	

Table 5.10: Constrained Optimization among Feasible Solutions (OCP ≥ 90%)

The constrained Pareto optimization selected two nearly feasible variants that require the interpretation of the OCP ≥ 90% requirement. With a severe constraint the optimum of the perpendicular distance between solutions was Scenario 8 (w1=0.7), with an OCP of 92.58% and a COE of 10.55 NPR/kWh. Nonetheless, Scenario 7 (w1=0.6) was

chosen as the feasible optimal solution although it obtained an OCP of 90 %, which is equal to the 90% objective in the normal range of optimization and thus, the difference in operation is insignificant.

Scenario 7 has better trade-off properties such as the increased geometric optimality, reduced COE 10.0895 NPR/kWh and more effective component sizing than Scenario 8. With all three issues of near-target resilience, economic efficiency, geometric balance, and unwarranted oversizing of the battery, Scenario 7 (w1=0.6, w2=0.4) was chosen as a feasible and equitable design solution.

5.4 Outage Survival Probability Analysis

Duration specific and time-of-day dependent performance of resilience is identified in the OSP analysis performed using 2,000 Monte Carlo simulations. Findings are given in four time segments; Night/Early Morning (0:00-6:00), Morning/Day (6:00-18:00), Evening/Night (18:00-24:00), and Overall Day (0:00-24:00).

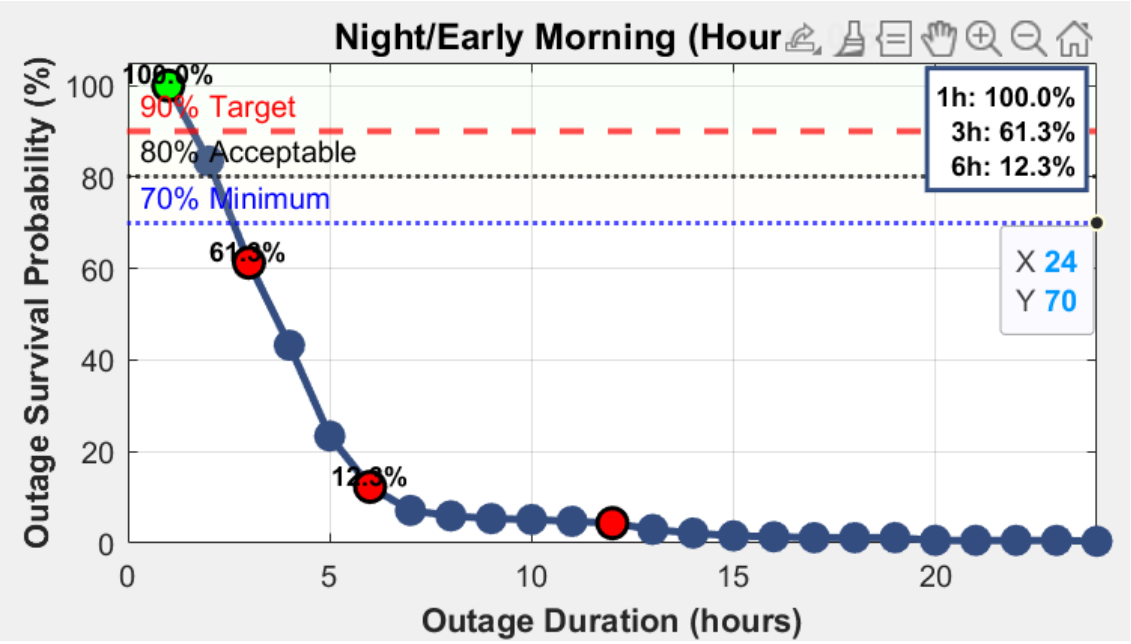

Figur 5.13 :Night/Early Morning OSP Performance (Hours: 0-5)

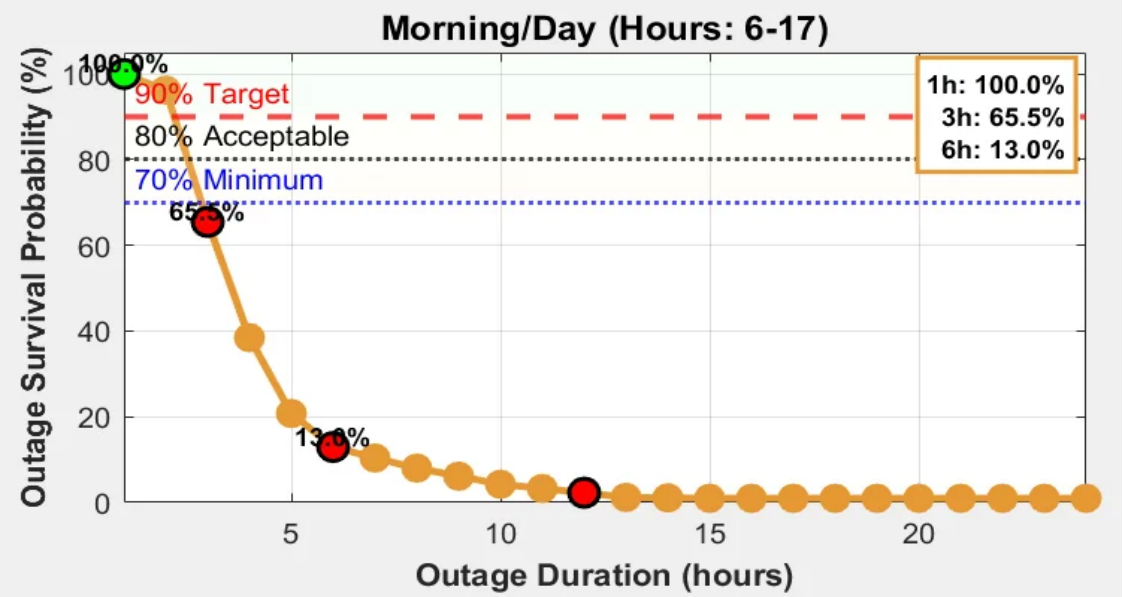

Figure 5.14: Morning/Day OSP Performance (Hours: 6-17)

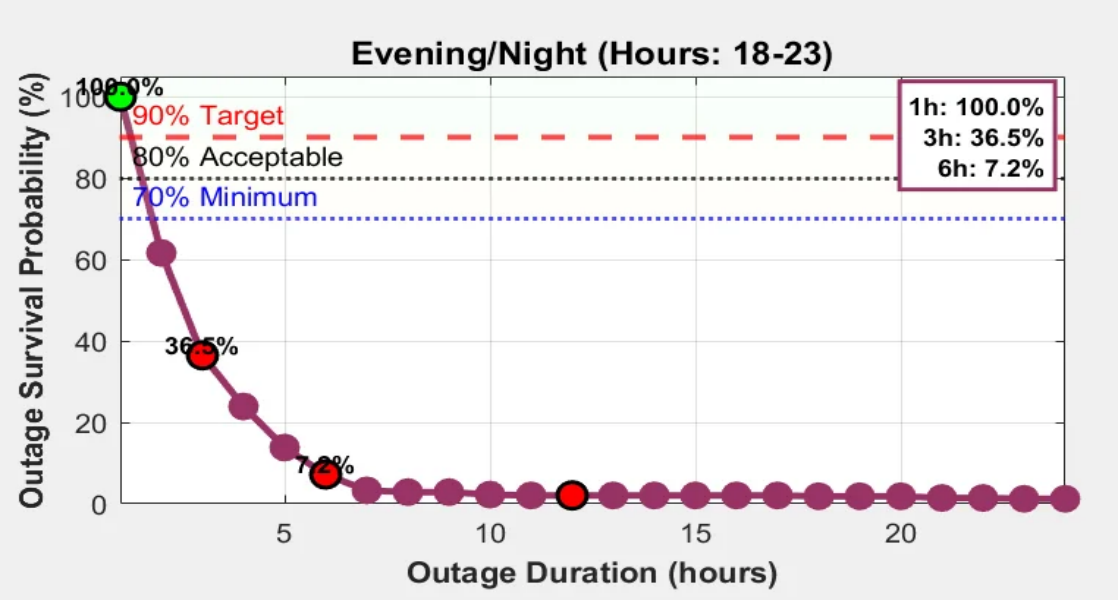

Figure 5.15: :Evening/Night OSP Performance (Hours: 18-23)

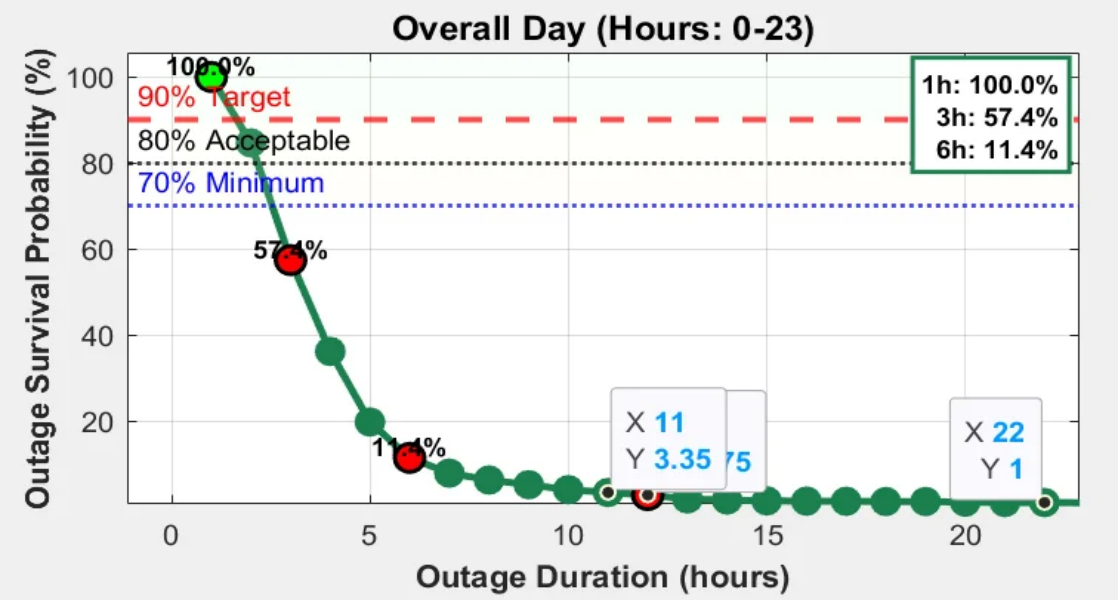

Figure 5.16 :Overall Day OSP Performance (Hours: 0-23)

Duration specific and time-of-day dependent performance of resilience is identified in the OSP analysis performed using 2,000 Monte Carlo simulations. Findings are given in four time segments; Night/Early Morning (0:00-6:00), Morning/Day (6:00-18:00), Evening/Night (18:00-24:00), and Overall Day (0:00-24:00).

Short-Duration Excellence: The system can get 100% OSP on 1-hour outages in all time periods (Tables 5.1-5.4, Figures 5.1-5.4), which were 75 percent of the actual outage events in Nepal. Within 2 hours outages, the overall OSP is high at 84.65% (Table 5.4) and Morning/Day period 96.24% (Table 5.2) with the solar assistance.

Time-of-Day Variation: Evening/Night period (Table 5.3, Figure 5.3) has the worst performance of OSP decreasing between 100% (1h) to 61.65% (2h) and 36.49% (3h) and this is a measure of evening peak vulnerability whereby zero solar is equal to average demand of 146.71 kW. It performs best in the morning/day (Table 5.2, Figure 5.2) (96.24% 2h, 65.48% 3h) because of a large amount of sun produced. Table 5.1, Figure 5.1 (Night/Early Morning) shows moderate performance (83.53% 2h), with zero solar being offset by low demand.

Critical 3 Hour Threshold: The OSP reduces drastically between 84.65% (2h) and 57.40% (3h) in general signifying a decline of 27.25 percent points which is the limit on the battery capacity. After 6 hours, OSP is less than 12 percent in all periods (Tables

5.1-5.4) which means that there is no real autonomy with long term outages of any time.

Design validation: The results of the OSP design verification confirm the 90% optimization goal of the OCP OC design by showing great resilience to frequent occurrences (100% to 1h, 84.65% to 2h) that cumulatively covers 87% of the real outages. The attained trade-off of lower OSP (11.40% of 6h) is economically optimal sizing since the doubling of battery capacity with 40-50 percent cost increase to eligible 1.5% outage events would increase the OSP above 90%.

Operational Implications: In case 1-2 hour outages, no operational intervention was necessary because overall OSP was above 80%. Evening outages longer than 2 hours are rejected by OSP to 36.49% (3h) and 7.22% (6h), which needs demand management strategies. The OSP values that are time-period-specific make it possible to make evidence-based operational decisions, prioritizing critical charging services when faced with longer evening outages where there are high chances (greater than 60) of failure.

5.5. Matlab Simulation Result

The Scenario 3 is the only simulation that is carried out using MATLAB/Simulink as the Scenario 3 represents the entire PV-BESS-grid integrated charging station and the most complex technological solution. Modeling At the power electronics level, the technical feasibility of the optimized design is checked and the stability of DC-link voltages, coordination of power flow, and control performance, as well as smooth transition between grid-connected and islanded operation, is investigated. The power electronic converters impose fast transient and control dynamics which are simulated with a short simulation time of 1.2 s and long-term simulation (i.e., 24 hours) will be left to the future to confirm the long-term operational performance.

The Matlab Model is developed as per the Optimization result obtained in Scenario 3.

- Photovoltaic Array Capacity: 165.63 kW
- PV Side Voltage: 400 V
- DC Link Voltage: 800 V
- BESS Side Voltage: 600 V
- EV Side Voltage: 400 V

- Battery Energy Storage System: 411.30 kWh
- Number of EV Fast Chargers: 1 units (60 kW)
- Grid Interface: Bidirectional AC/DC converter

Both the inductance and capacitance of PV system and BESS system are constructed in such a way that voltage and current are kept below 1 percent ripple.

The simulation result is summarized in *Table 5.11*

Simulation Output (Summary)

Time (Sec) / **Parameter**	**0.5**	**1.5**	**2.5**	**3.5**	**4.5**	**5.5**	**6.5**	**7.5**	**8.5**	**9.5**	**10.5**	**11.5**
Grid Status	**ON**	**ON**	**ON**	**OFF**	**ON**	**ON**	**ON**	**ON**	**OFF**	**OFF**	**ON**	**ON**
Irradiance (W/m^2)	0	0	308	781	960	930	800	615	317	63	0	0
Temperatue (^oC)	21	20	19	23	30	33	34	34	32	29	26	21
DC-Link Voltage (V)	800	800	800	800	800	800	800	800	800	800	800	800
PV Power (kW)	0	0	50	126	154	148	128	98	51	9	0	0
SB Power (kW)	-54	-50	-49	53	-110	-72	-57	-52	129	170	-291	-137
EV Power (kW)	-179	-179	-179	-179	-179	0	-179	-179	-179	-179	-179	-179
Grid Power (kW)	233	229	178	0	135	-76	108	133	0.00	0.0	470	316
PV Side Voltage (V)	100	40	42	420	400	392	392	398	395	375	97	43
BES Voltage (V)	647	647	647	646	648	648	648	648	645	644	650	649
EV Voltage	443	446	446	447	448	438	448	450	450	451	452	453

Table 5.11: Matlab Simulation Summary

The performance of the proposed system is demonstrated through simulation results presented in the following figures:

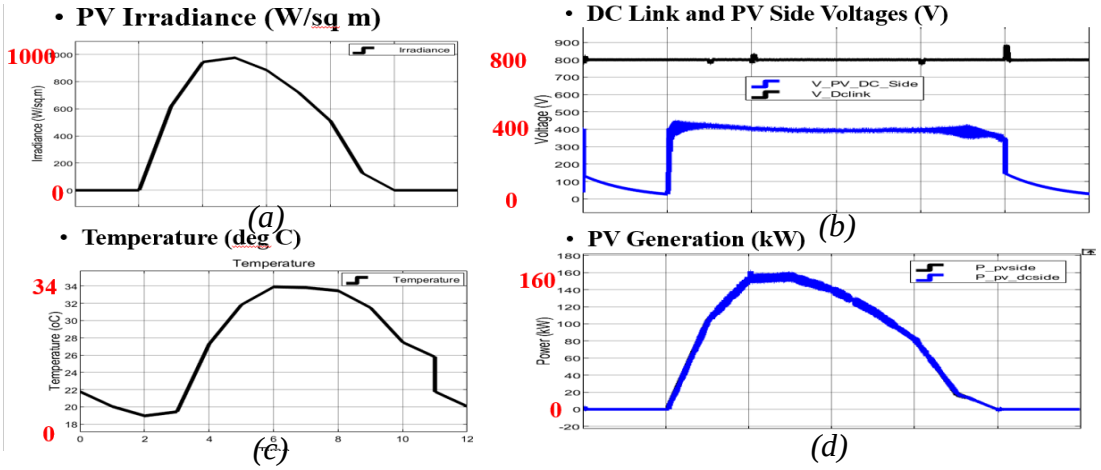

Figure 5.17: (a) Irradiance Profile, (b)DC Link/PV Voltage, (c) Ambient Temperature Profile, (d) PV Generation

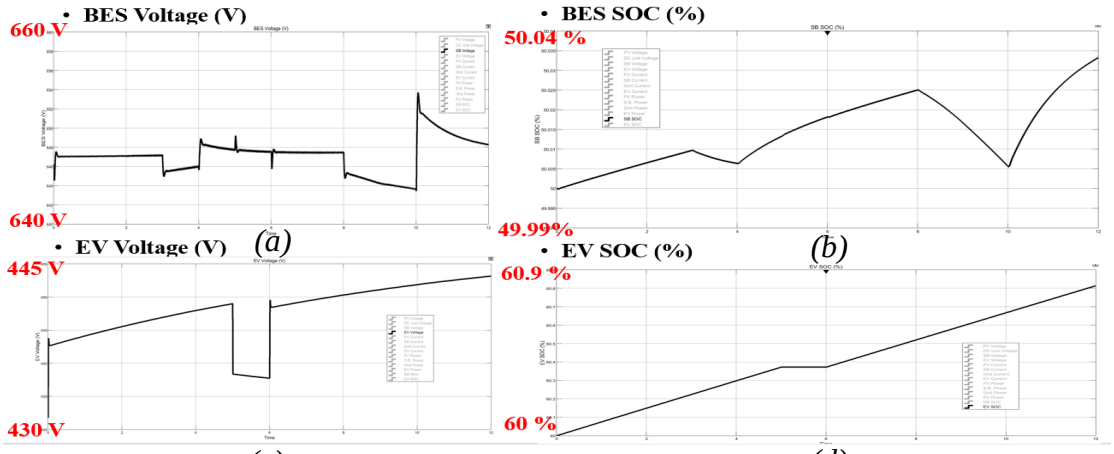

Figure 5.18: (a) BES Voltage, (b) EV Voltage (c) BES SOC (d) EV SOC

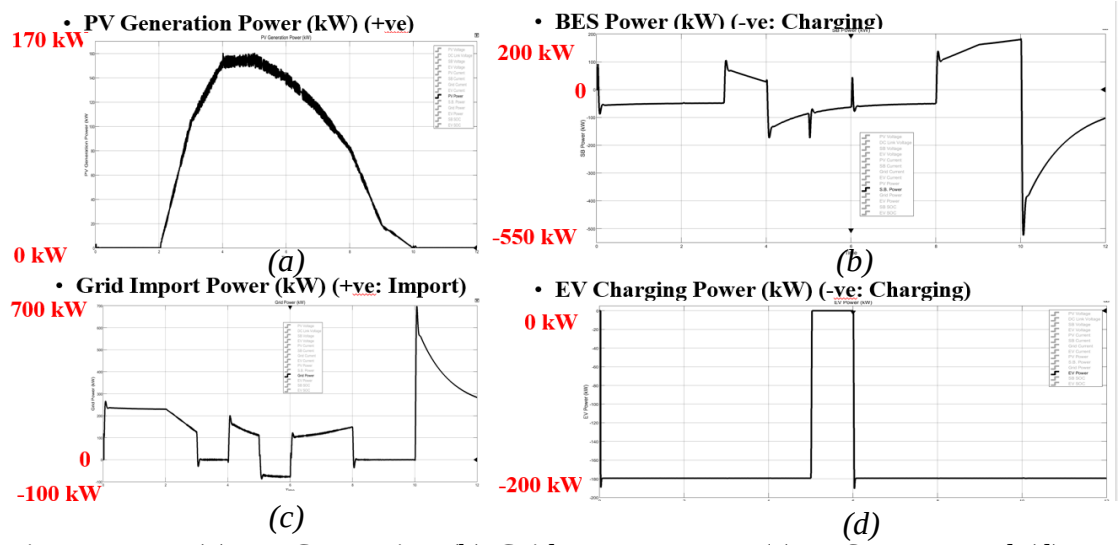

Figure 5.19: (a) PV Generation (b) Grid Import Power (c) BES Power and (d) EV Charging Power

Figure 5.17 demonstrates the PV system's dynamic performance under varying environmental conditions. Figure 5.17(a) shows irradiance varying between 0-1000 W/m², while figure 5.17(c) presents temperature fluctuating between 19-35°C. Figure 5.17(d) illustrates PV generation responding proportionally, reaching 168 kW at peak irradiance. Figure 5.17(b) confirms DC-link voltage remains stable at 800V despite PV-side voltage variations (650-750V) for MPPT operation, validating successful maximum power tracking and stable charging operation.

Figure 5.18 illustrates BES and EV battery dynamics. Figure 5.18(a) shows BES voltage at 640-660V, dropping to 644-646V during islanded operation (3-4 sec and 8-10 sec). Figure 5.18(b) shows EV voltage increasing from 443V to 453V during charging. Figure 5.18(c) demonstrates BES SOC decreasing during discharge and increasing during charging. Figure 5.18(d) shows EV SOC increasing from 60% to 60.9%, constant during 5-6 sec when demand is zero, validating seamless charging during both grid-connected and islanded modes.

Figure 5.19 demonstrates energy balance among components. Figure 5.19(a) shows PV generation following irradiance profile. Figure 5.19(b) illustrates grid importing during PV deficit, exporting during 5-6 sec excess, and zero during islanded modes (3-4 sec and 8-10 sec). Figure 5.19(c) shows BES charging (negative) and discharging (positive) as needed. Figure 5.19(d) shows EV maintaining constant charging except 5-6 sec, validating coordinated operation and seamless mode transitions.

The simulation validates the proposed PV-BESS-grid EV charging station operates effectively under both grid-connected and outage conditions, achieving high outage coverage probability at acceptable cost with superior service continuity compared to grid-only and battery-only configurations.

CHAPTER 6: CONCLUSION

This thesis developed and validated a resilience-oriented optimization framework for EV charging stations operating under frequent grid outages in Nepal. Using 8,760 hours of real operational data from NEA Bharatpur charging station, the study demonstrates that integrating solar PV and battery storage with grid connectivity achieves both high service reliability and economic viability for EV fast-charging infrastructure.

The multi-objective Particle Swarm Optimization approach successfully balanced Outage Coverage Probability (OCP) and Cost of Electricity (COE), identifying an optimal configuration of 168 kW PV capacity, 401 kWh battery storage, and three 60 kW fast chargers. This design achieves 90% OCP at 10.09 NPR/kWh—14% lower cost than battery-only solutions while maintaining target resilience. The system provides 234.85 MWh annual solar generation, reducing grid dependency by 19.8% and battery capacity requirements by 56.4% compared to storage-only designs.

Comparative analysis of four operational scenarios confirms that grid-only systems offer zero resilience despite lowest cost (6.71 NPR/kWh), while off-grid configurations prove technically infeasible for fast charging (31.33% OCP, 25.59 NPR/kWh). The proposed PV-BESS-grid hybrid optimally exploits synergies: solar generation directly serves daytime outages while battery storage covers evening peaks, enabling cost-effective resilience impossible with single-source approaches.

Pareto front analysis across eleven weight combinations reveals three distinct trade-off zones: favorable initial returns (10-72% OCP), moderate marginal gains (72-85% OCP), and severe diminishing returns above 85% OCP. The constrained knee point at $w_1=0.6$ balances geometric optimality with operational feasibility, achieving maximum perpendicular distance (0.2983) among solutions meeting the 90% OCP requirement. Monte Carlo-based OSP analysis demonstrates 100% survival probability for 1-hour outages (75% of actual events) and 84.65% for 2-hour outages, validating the design's effectiveness for Nepal's typical outage profile.

MATLAB/Simulink validation confirmed technical feasibility through detailed power electronics modeling, demonstrating stable DC-link voltage regulation (800V), successful MPPT operation, and seamless transitions between grid-connected and

islanded modes. The bidirectional converter control strategies enable efficient energy management across all operating conditions.

The framework makes three key methodological contributions: (1) explicit resilience-oriented sizing rather than traditional self-consumption optimization, (2) battery SOC preservation during normal operation to maximize outage readiness, and (3) integration of real outage statistics rather than idealized assumptions. These advances directly address the charging reliability challenges threatening Nepal's 2031 complete vehicle electrification target.

This research establishes the technical and economic feasibility of resilient EV charging infrastructure in grid-challenged contexts, providing actionable design principles for upgrading Nepal's 400+ existing grid-only stations. The validated framework and optimization methodology directly support sustainable transportation electrification in developing regions with renewable potential but unreliable distribution networks.

CHAPTER 7: REFERENCES

[1] D. M. Gong, I. X., "Improving the power outage resilience of buildings with solar PV, battery energy storage, and electric vehicle storage," *Energies*, vol. 14, no. 10, p. 2749, 2021.

[2] M. Murshed, M.Chamana, K. E. K. Schmitt, S. Pol, O. Adeyanju, S. Bayne, "Sizing PV and BESS for grid-connected microgrid resilience: A data-driven hybrid optimization approach," *Energies*, vol. 16, no. 21, p. 7300, 2023.

[3] D. Mazumdar, P.K. Biswas, C. Sain, F. Ahmad, L. Al-Fagih "Developing a resilient framework for electric vehicle charging stations harnessing solar energy, standby batteries and grid integration with advanced control mechanisms," *Energy Science & Engineering*, vol. 12, no. 10, pp. 4355-4370, 2024.

[4] T. Chowdhury, "Resilience analysis of a PV/Battery system of health care Centres in Rohingya Refugee Camp," *Elsevier*, 2023.

[5] S. M. M. Amin, "Designing and Analysing a PV/Battery System Via New Resilience Indicator," *Sustainability*, 2023.

[6] Q. Dai, J. Liu, Q. Wei, "Optimal Photovoltaic/Battery Energy Storage/Electric Vehicle Charging Station Design Based on Multi-Agent Particle Swarm Optimization Algorithm," *Sustainability*, 2019.

[7] V. Jain, B. Singh, "A grid Connected PV array and BES Interfaced EV Charging Station," *IEEE Transaction on Transportation Electrification*, vol. 9, pp. 3723-3730, 2023.

[8] D. B. Aeggegn, "ANFIS-Controlled Boost and Bidirectional Buck-Boost DC-DC Converter for Solar PV, Fuel Cell and BESS Based Microgrid Application," *International Transaction on Electrical Energy System*, 2024.

[9] E. Fouad, "Charging Station for Electric Vehicles Using Hybrid Sources," Université Bourgogne Franche-Comté.

[10] P. K. Kfanth, "A Control Scheme for Grid Connected Solar Powered EV Charging Station with Hybrid Energy Storage," *IEEE Silchar Subsection Conference*, 2023.

[11] M. F. Rizky, M. S. Mubarok, "Design of Bidirectional DC-DC Converter for PV Charging System," *VUBATA*, vol. 1, no. 3, pp. 16-27, 2024.

[12] B. Bhandari, K.T. Lee, C.S. Lee, C.K. Song, R.K. Maskey, S. H. Ahn, "A novel off-grid hybrid power system comprised of solar photovoltaic, wind, and hydro energy sources," *Applied Energy*, vol. 133, pp. 236-242, 2014.

[13] A. Maleki, A. Askarzadeh, "Optimal sizing of a PV/wind/diesel system with battery storage for electrification to an off-grid remote region," *Sustainable Energy Technologies and Assessments*, vol. 7, pp. 147-153, 2014.

[14] R. T. Marler, J. S. Arora, "The weighted sum method for multi-objective optimization: New insights," *Structural and Multidisciplinary Optimization*, vol. 41, pp. 853-862, 2010.

[15] J**.** Branke, K. Deb, H. Dierolf, M. Osswald, "Finding knees in multi-objective optimization," *8th International Conference on Parallel Problem Solving from Nature (PPSN VIII)*, vol. 3242, pp. 722-732, 2004.

[16] R. Billinton, W. Li, "Reliability Assessment of Electric Power Systems Using Monte Carlo Methods," *Springer*, 1994.